RESEARCH ARTICLE | NOVEMBER 11 2024

Influence of temperature and crack-tip speed on crack propagation in elastic solids

B. N. J. Persson

J. Chem. Phys. 161, 184704 (2024)
https://doi.org/10.1063/5.0236699

The Journal of Chemical Physics ARTICLE pubs.aip.org/aip/jcp

Influence of temperature and crack-tip speed on crack propagation in elastic solids

Cite as: J. Chem. Phys. 161, 184704 (2024); doi: 10.1063/5.0236699
Submitted: 1 September 2024 • Accepted: 20 October 2024 •
Published Online: 11 November 2024

B. N. J. Persson[a)]

AFFILIATIONS

State Key Laboratory of Solid Lubrication, Lanzhou Institute of Chemical Physics, Chinese Academy of Sciences, 730000 Lanzhou, China; Peter Grünberg Institute (PGI-1), Forschungszentrum Jülich, 52425 Jülich, Germany; and Multiscale Consulting, Wolfshovener Str. 2, 52428 Jülich, Germany

[a)]Author to whom correspondence should be addressed: b.persson@fz-juelich.de

ABSTRACT

I study the influence of temperature and the crack-tip velocity of bond breaking at the crack tip in rubber-like materials. Bond breaking is considered as a stress-aided thermally activated process and results in an effective crack propagation energy, which increases strongly with decreasing temperature or increasing crack-tip speed. This effect is particularly important for adhesive (interfacial) crack propagation but less important for cohesive (bulk) crack propagation owing to the much larger bond-breaking energies in the latter case. For adhesive cracks, the theory results are consistent with adhesion measurements for silicone rubber polydimethylsiloxane (PDMS) in contact with silica glass surfaces. For cohesive cracks, the theory agrees well with experimental results PDMS films chemically bound to silanized glass.

I. INTRODUCTION

Crack propagation in rubber-like materials is a topic of great importance and is involved in many practical applications, such as the wear of tires or conveyor belts.[1,2] The energy to propagate an opening crack over a surface area ΔA in viscoelastic solids depends on the temperature T and the crack-tip velocity v and is usually written as $G(v,T)\Delta A$. We will, for simplicity, denote $G(v,T)$ as the "crack-energy." The crack energy is usually written as[3–11]

$$G(v,T) = G_0(v,T)[1 + f(v,T)]. \tag{1}$$

Here, the factor $[1 + f(v,T)]$ with $f \geq 0$ is attributed to viscoelastic energy dissipation in a region, which can extend far from the crack tip,[12–26] and $G_0(v,T) = g(v,T)G_{00}$ with $g \geq 1$ is due to the bond breaking in the crack-tip process zone. Here, G_{00} is the change in the free energy per unit surface area to separate the surfaces at the crack tip and $g(v,T)$ is a non-adiabatic factor, which will be studied in this paper. For cohesive cracks (cracks propagating inside the rubber), recent studies[27] have shown that the bond breaking may start far from the crack tip, and in these cases, there may be no clear separation between the process zone and the viscoelastic dissipation zone. For adhesive crack propagation at the interface between a viscoelastic solid and a counter surface, the stresses may be much smaller than for cohesive crack propagation, and in these cases, there may be a negligible overlap between the two spatial regions, but I am not aware of experimental studies addressing this topic.

In the present study, I will assume that there is negligible viscoelastic energy dissipation and focus on the velocity and temperature dependency of the $G_0(v,T)$ factor in (1). Silicone rubber has a very low glass transition temperature ($T_g \approx -120\,^\circ$C). At room temperature, and for typical crack-tip speeds, polydimethylsiloxane (PDMS) rubber is usually considered as a nearly perfect elastic material, but adhesive crack propagation still shows some viscoelastic effects (see Fig. 1 and Ref. 28).

In the following, we focus mainly on the velocity dependency of the crack-energy, and we denote $G(v,T)$ by $G(v)$ for simplicity. In Fig. 1(a), the square symbols are the measured crack-energy $G(v) = G_0(v)[1 + f(v)]$ and (b) $G_0(v)$ as a function of the crack-tip velocity v, for PDMS in contact with silica glass at $T = 20\,^\circ$C. The green lines are the calculated $[1 + f(v)]$ factor for different temperatures assuming a constant (velocity independent) $G_0(v) = G_{00}$. The lowest green line is for $T = 20\,^\circ$C. It agrees well with the measured data for $v < v_c \approx 0.1$ mm s^{-1}. Similar results were obtained in Refs. 36 and 37 and in Ref. 38 for PDMS with other cross-link densities. The abrupt increase in $G(v)$ for $v > v_c$ should be noted. We

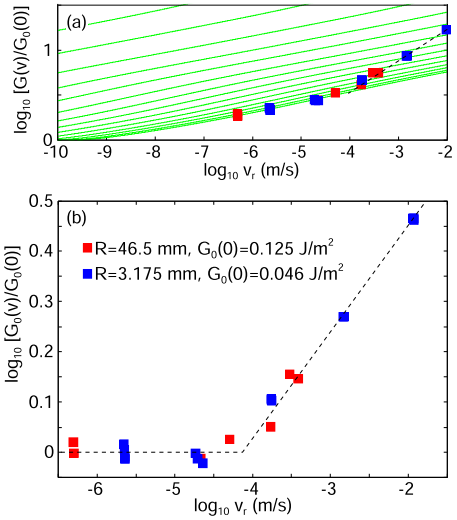

FIG. 1. Square symbols are the measured crack-energy $G(v) = G_0(v)[1 + f(v)]$ (a) and $G_0(v)$ (b) as a function of the crack-tip velocity v (log–log scale) for a polydimethylsiloxane (PDMS) rubber (Sylgard 184, 1:10 cross-linker/base) at $T = 20\,^{\circ}\mathrm{C}$. The green lines are the calculated $[1 + f(v)]$ factor assuming a constant (velocity independent) $G_0(v) = G_{00}$. The lowest green line is for $T = 20\,^{\circ}\mathrm{C}$, and the other lines are for 10, 0, . . ., −110 °C; adapted from Ref. 35.

will show that for $v < v_c$, the crack-energy $G_0(v) = G_{00}$ is the thermal equilibrium bond-breaking energy, while for $v > v_c$, the bond breaking occurs in a non-adiabatic way, resulting in an increase in $G_0(v)$ with increasing v.

At very low crack-tip speeds, bonds are broken by thermal fluctuations rather than by the applied force. For this case, the breaking of adhesive bonds may require relative small energies, which can be estimated from the low-velocity (adiabatic) crack-energy $G_0(v \to 0) = G_{00}$, which for silicone rubber against a silica glass surface may be of the order ~0.1 $\mathrm{J/m^2}$ or ~0.6 $\mathrm{eV/nm^2}$. Assuming that the bonding area is of the order ~1 $\mathrm{nm^2}$, this gives effective bond energies of the order ~0.6 eV. It should be noted that this is larger than expected for a single van der Waals bond; the detached surface area is not of the size of a single atom but most likely a nanometer sized patch of the rubber. For cohesive cracks, strong covalent bonds are broken at the crack tip, which may require ~3 eV. For this case, the effective energy to break bonds will increase with the crack-tip speed already at very low crack-tip speeds, while for PDMS at room temperature, this occurs only for relative large crack-tip speeds of order 0.1 mm $\mathrm{s^{-1}}$ (see Fig. 1).

Thermally activated, stress-aided bond breaking will also manifest itself in non-steady crack propagation, even for purely elastic solids. Therefore, at non-zero temperature, a strip of rubber with a crack will fracture in two fragments at a higher applied stress if the strip is elongated fast compared to slow elongation rate. This result is due to the influence of thermal excitation, which is more important during slow elongation than during fast elongation.

In a fundamental study, Lake and Thomas[40] have shown that in highly elastic materials, for cohesive cracks, the crack energy may be strongly enhanced (by a factor up to ~100) compared to its (hypothetical low-velocity) adiabatic value G_{00} (which may never be observed experimentally as it requires velocities lower than can ever be reached on the time scale of human activities). They showed that this enhancement is due to the stretching of polymer chains before breaking the strong covalent bonds (see Fig. 2). This effect is also important for adhesive cracks but in these cases only for much higher crack-tip speeds, e.g., above 0.1 mm $\mathrm{s^{-1}}$ for PDMS against silica glass.

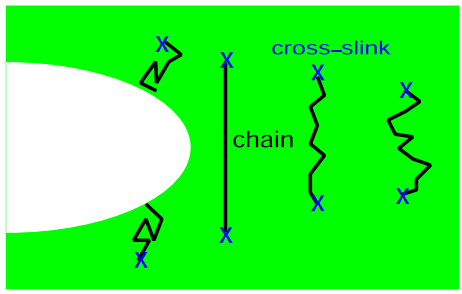

FIG. 2. Lake and Thomas explanation of the high crack-energy of rubber-like materials. When the crack-tip approach a chain molecule (consisting of N monomers or bond-units between the cross-links), extending over the (to be) fracture plane, the chain stretches and at the point when one bond breaks, the stored up energy is N times the energy required to break one bond.

In this paper, I study the influence of temperature and the crack-tip velocity of the bond breaking at the crack tip in rubber-like materials. The bond breaking is considered as a stress-aided thermally activated process. The model results in an effective crack energy, which increases strongly with decreasing temperature or increasing crack-tip speed. The analysis includes the chain-stretching effect of Lake and Thomas and results in a $G_0(v, T)$, which is consistent with experimental observations. I note that stress-aided thermally activated processes are involved in nearly all applications, where bonds are broken, e.g., in sliding friction,[41–45] and goes back to the theories of Prandtl[42] (also see Refs. 44 and 45) and Eyring[46] for the dependency of the strength of solids (plasticity) and fluids (viscosity) on the temperature and the deformation rate. Other related works are theoretical (and atomic force microscopy) studies of the strength of single bonds.[47,48] Kendall[49] and Chaudhury[50–52] (also see Refs. 53–55) have suggested that stress-aided thermally activated bond breaking may also be important for adhesive cracks.

II. CRACK PROPAGATION IN A LONG SLAB–ENERGY METHOD

Consider an elastic rectangular block with the length L much larger than the height h_0 in adhesive contact with a substrate. We assume that the upper surface of the slab is clamped and displaced by Δh, as shown in Fig. 3.

Adhesive crack propagation occurs at the interface between an elastic block (or film) and another solid (substrate), which can usually be considered as rigid, as shown in Fig. 3(a). In this case, the crack-energy G will involve breaking the adhesive bonds at the interface between the solids, and the elastic energy U_{el} is stored mainly in the upper (elastic) block. For *cohesive* crack propagation

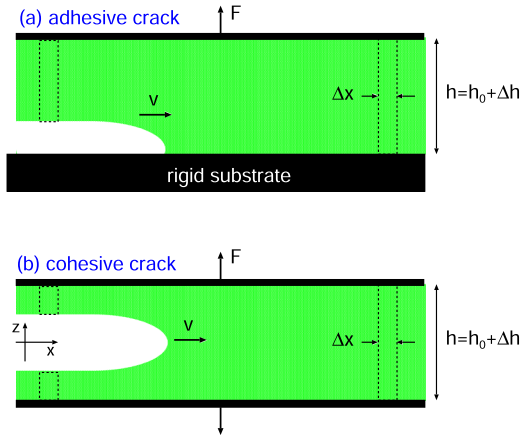

FIG. 3. (a) Adhesive crack: a crack at the interface between a rigid substrate and an elastic block in adhesive contact with the substrate (adhesive crack). The rectangular elastic block has the length L, height h_0, and width (not shown) w. We assume $L \gg h_0$ and $h_0 \gg w$. The top surface of the block is clamped (glued to rigid plate, upper black region) and displaced so the height of the block increases with Δh. The stress in the block far in front of the crack is $\sigma_0 = E\epsilon$, where the strain $\epsilon = \Delta h/h_0$. The stress far behind the crack tip vanishes. (b) Cohesive crack: a crack occurs in the middle of the elastic block.

[see Fig. 3(b)], the upper $z > 0$ and lower $z < 0$ part of the solid block are the same.

Assume that a crack occurs for $x < 0$ and that the crack is much longer than the height h_0 of the slab. A segment of the block of width Δx for $x \gg h_0$ will experience a uniform strain $\epsilon_0 = \Delta h/h_0$ and the stress $\sigma_0 = E\epsilon_0$ so that the elastic deformation energy stored up in the segment is

$$U_{\rm el} = \frac{1}{2}\sigma_0\epsilon_0\Delta V = \frac{1}{2E}\sigma_0^2\Delta V,$$

where $\Delta V = h_0 w\Delta x$ is the volume of the segment (w is the width of the slab into the paper plane). Far behind the crack tip (for $x \ll -h_0$), the strain and the elastic energy in a segment of width Δx both vanish. If the crack moves forward with a distance Δx, the bonds between the atoms must be broken over an area $\Delta A = w\Delta x$. If G denotes the energy to break the bonds per unit surface area, then the fracture energy is

$$U_{\rm ad} = Gw\Delta x.$$

In order for the crack to be able to move forward, the reduction in the stored elastic energy must be (at least) the energy needed to break the interfacial bonds or $U_{\rm el} = U_{\rm ad}$ giving

$$\sigma_0 = \left(\frac{2GE}{h_0}\right)^{1/2}. \tag{2}$$

III. CRACK PROPAGATION IN A LONG SLAB–STRESS METHOD

The stress field in the vicinity of crack tips depends on the distance r from the crack tip as $\sim r^{-1/2}$. This result is very general and holds for static cracks, moving cracks, and cracks in viscoelastic

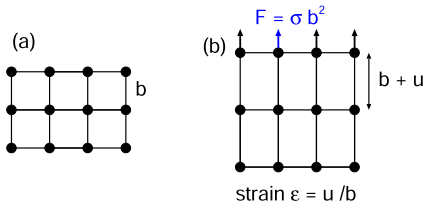

FIG. 4. When a rectangular block is elongated by a stress σ, the bonds between the atom stretch by u so the strain $\epsilon = u/b$. The bond breaks when the displacement u is of order b. The strain and stress at the point of bond fracture are $\epsilon_c \approx 1$ and $\sigma_c = E\epsilon_c \approx E$, respectively.

solids. In ideal brittle solids, for low crack-tip speeds, the singular stress field $\sim r^{-1/2}$ holds down to atomic distances from the singularity. For the crack shown in Fig. 3, we expect the stress at a distance $\sim h_0$ in front of the crack tip to be of the order of the applied stress σ_0 so that[56]

$$\sigma(r) \approx \sigma_0\left(\frac{h_0}{2r}\right)^{1/2}.$$

In order to break the bonds at the crack tip, the stress for $r \approx a_0$, where a_0 is an atomic distance, must equal the stress σ_c to break bonds so that

$$\sigma_c \approx \sigma_0\left(\frac{h_0}{2a_0}\right)^{1/2}$$

or

$$\sigma_0 \approx \sigma_c\left(\frac{2a_0}{h_0}\right)^{1/2}. \tag{3}$$

For cohesive cracks, when assuming no plastic deformation, $\sigma_c \approx E$ (see Fig. 4). This gives

$$\sigma_0 \approx E\left(\frac{2a_0}{h_0}\right)^{1/2}. \tag{4}$$

Next, it should be noted that the work per unit surface area to break the bonds is $G \approx Ea_0$. Using this result in (4) gives

$$\sigma_0 \approx \left(\frac{2E^2a_0}{h_0}\right)^{1/2} \approx \left(\frac{2GE}{h_0}\right)^{1/2},$$

which is the same result as (2). It should be noted that this result is obtained only if the stress at the crack tip varies as $\sim r^{-1/2}$, which supports the statement that the stress close to the crack tip has this singular form.

IV. DISCUSSION

We have shown that the energy and stress methods used above give the same results when applied to cohesive cracks, assuming no plastic deformations. However, when applied to adhesive cracks, they result in a paradox or mystery, as we will now show. Consider an interfacial crack and assume that (2) and (3) are both valid. This implies

$$\sigma_0 = \left(\frac{2GE}{h_0}\right)^{1/2} = \sigma_c\left(\frac{2a_0}{h_0}\right)^{1/2}. \tag{5}$$

From (5), we get

$$a_0 = \frac{GE}{\sigma_c^2}. \tag{6}$$

If F_c is the force to break an adhesive bond, and $n_0 = 1/b^2$ the concentration of bonds, then $\sigma_c = F_c/b^2$. Since $F_c \approx Gb^2/a$, where a is an atomic length, we get $\sigma_c \approx G/a$ and from (6),

$$a_0 = \frac{GE}{\sigma_c^2} \approx \frac{Ea^2}{G}. \tag{7}$$

Now, the force to break an adhesive bond is, in general, independent of the elastic modulus E, and it is clear from (6) or (7) that a_0, *in general, cannot be an atomic distance* since Young's modulus E can take a wide range of values. We will illustrate the problem with two practical cases.

First, consider an adhesive crack between two flat diamond (111) surfaces, where the dangling bonds are passivized by hydrogen atoms [self-mated C(111)(1 × 1)H]. The work of adhesion for this system is $G \approx 0.2$ J/m^2 (see Ref. 57), the Young's modulus of diamond $E \approx 1.2 \times 10^{12}$ Pa and using the atomic distance $a \approx 0.3$ nm from (7), we get

$$a_0 \approx \frac{Ea^2}{G} \approx 5\ \mu\text{m}.$$

Hence, the bond-breaking occurs a long distance away from where the stress singularity occurs in the continuum approximation. We attribute this to the large modulus of diamond and small work of adhesion of the passivized diamond surface, which will make the diamond surfaces nearly parallel, and separated by an atomic distance, in a large region behind the crack tip. This makes the point, where a bond break, is somewhat undefined. In any case, the fact that a_0 is large is not associated with any physical problem.

One could argue that the energy method of Sec. II is better than the stress method of Sec. III because there is no direct way to determine a_0. However, both approaches depend on only one quantity, which in most cases need to be determined experimentally. In the energy approach, this is the crack-energy G (or rather EG) and in the stress approach, the parameter $\sigma_c\sqrt{a_0}$. These parameters could both be determined experimentally using a simple setup such as the long-slab configuration studied above. With G or $\sigma_c\sqrt{a_0}$ known, crack propagation in more complex situations could be studied as usual by calculating the relevant stress intensity factors. In some cases, as for the hydrogen-passivized diamond surfaces, it is possible to calculate (or estimate) G from first principle using quantum mechanical methods (e.g., see Ref. 57), while it is less clear how to determine $\sigma_c\sqrt{a_0}$ theoretically if not obtained indirectly from (6).

Next, consider a rubber block adhering to a flat, rigid substrate. As an example, first consider a fully cross-linked Polydimethylsiloxane (PDMS, Sylgard 184) rubber adhering to a glass surface. In this case, $E \approx 2 \times 10^6$ Pa and $G \approx 0.1$ J/m^2 (e.g., see Refs. 35 and 38), and (7) gives

$$a_0 \approx \frac{Ea^2}{G} \approx 10^{-13}\ \text{m}.$$

Hence, a_0 is much smaller than an atomic length, which is impossible. To discuss this paradox, first note that using $a_0 = 0.3$ nm in (6), the stress at the crack tip,

$$\sigma_c = \left(\frac{GE}{a_0}\right)^{1/2} \approx 26\ \text{MPa}.$$

Using $E = 2 \times 10^6$ Pa, this corresponds to the strain $\epsilon \approx \sigma_c/E \approx 13$. It is clear that linear elasticity theory will fail close to the crack tip even for the relative weak adhesion considered here. The stress–strain curve for large strain for PDMS is (highly) nonlinear, with the stress increasing much faster than linearly with increasing strain as polymer chains approach their fully stretched state. For PDMS Sylgard 184, the yield stress in tension for the perfect (defect free) block may be larger than the critical stress $\sigma_c \approx 26$ MPa found above, in which case, the rubber at the crack tip would respond as a nonlinear elastic material but without breaking cross-links and without the formation of defects such as cavities. This conclusion is also supported by the result shown in Fig. 5: as long as the substrate bond (which typically is of the van der Waals nature, and hence very weak) is weaker than the cross-link bonds, one expects the polymer–substrate bond to break before the cross-link bonds break. However, for weakly cross-linked PDMS, the elastic modulus is much smaller (e.g., only 19 kPa for Sylgard PDMS produced by mixing cross-linker/base fluids in the ratio 1:50), and in these cases, the strain σ_c/E calculated from (6) with a_0 as an atomic distance would be huge and the rubber would break-up (e.g., cavitation and stringing) close to the crack tip. (In addition, weakly crosslinked rubbers have free chains, which could get pulled out during opening crack propagation.[58–60] This has been observed experimentally for the contact between a silica glass sphere and PDMS rubber. Here, the effective work of adhesion decreases with the number of contacts due to pullout and transfer of uncross-linked chains to the glass surface.[35,61–63])

The results presented above show that if a_0 calculated from (7) is smaller than an atomic length, the linear elastic theory cannot be used all the way down to atomic distances from the crack tip, but depending on the system, one needs to take the following into account:

(a) non-linear elasticity effects close to the crack tip, which may effectively increase the elastic modulus E, and hence also a_0, and
(b) plastic deformation, or the formation of defects, such as cavities or (for polymers) stringing, in a region close to the crack tip.

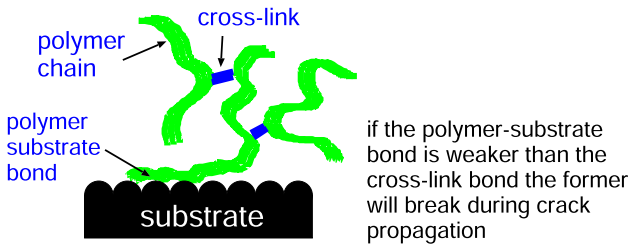

FIG. 5. Adhesive bonds are often of the weak van der Waals type. In these cases, for a covalent cross-linked polymer, the adhesion bonds will break before the chain or cross-links break.

In both cases, the effective a_0 would be larger than predicted by (7).

We note that for elastic solids, the cutoff distance a_0 and σ_c always enter in the combination $\sigma_c\sqrt{a_0}$ and it is usually not possible to measure σ_c and a_0 separately. The analysis above shows that if one chooses $\sigma_c^2 a_0 = G_0$, the stress theory will give the same result as the energy theory. However, for viscoelastic solids (denoted here as rubber), the situation is different. For very low sliding speeds (or high temperature), the rubber is in the rubbery region and behaves as an elastic solid and the crack propagation will only depend on the (low velocity) crack energy $G_0 = G(v \to 0)$, which we can write again as $\sigma_c\sqrt{a_0}$. However, as we increase the sliding speed, there will be viscoelastic energy dissipation in a region around the crack tip. A crack tip, which moves with the speed v, will generate time-dependent deformations of the rubber with a band of frequencies, $\omega \sim v/r$ $(a < r < \infty)$, where r is the distance from the crack tip. The highest frequency component is given by v/a, where $a = a(v)$ is the crack-tip cutoff length with $a \to a_0$ as $v \to 0$. Hence, the crack-energy $G(v)$ will now depend on *both* G_0 and a_0. The fracture energy G_0 can be directly measured experimentally, but the cutoff distance a_0 is not so easy to measure directly but could be deduced by comparing the measured $G(v)$ curve to the theory prediction (it should be noted that the $G(v)$ curve shifts along the velocity axis linearly with a_0). However, as shown above, if linear viscoelasticity is used, this could result in a cutoff length a_0, which would be unphysically small. This would signal that non-linear viscoelastic effects, or other phenomena such as cavitation, occur close to the crack tip.

For adhesive cracks, the stress field far from the crack tip, where most of the viscoelastic energy dissipation occurs, may be small enough for linear viscoelasticiy to be valid. However, when calculating (or estimating) the viscoelastic contribution to the crack energy for rubber-like materials, one must use for a_0, a length at least of order some monomers (say ~1 nm).

V. THERMAL EFFECTS ON CRACK PROPAGATION

Theories for cracks in solids often assume a crack-tip process zone, which can be very complex involving plastic flow, cavitation, stringing, and bond-breaking far from the crack tip. However, here we consider adhesive crack propagation and assume that the stress close to the crack tip is so small that only the (weak) interfacial bonds break. For weak bonds, thermal activation can be very important and result in the interfacial bonds breaking (and reforming) already far in front of the crack tip.

If the elastic energy $U_{el} > U_{ad}$, opening crack propagation occurs, while if $U_{el} < U_{ad}$, closing crack propagation occurs. For zero temperature, a crack will not move (stationary crack) if $U_{el} = U_{ad}$. However, for $T > 0$ cracks can move by thermal excitation even if $U_{el} = U_{ad}$. In this case, the crack length could increase or decrease, correspond to opening and closing crack propagation, and in general, the crack tip would perform a random, Brownian-motion type of movement.[64] However, in many practical situations when bonds break, some irreversible process occur, such as passivization of the dangling bonds by reaction with air or contamination molecules, or surface reconstruction, and in these cases, only opening crack propagation may occur. This could result in a slow increase in the crack length even when $U_{el} < U_{ad}$, as observed in stress corrosion cracking. We will study this problem in another publication.

A crack is a line defect and thermal excitations will result in different regions of a crack-line moving at different times resulting in a curved crack line. Thus, the energy barrier for movement of the crack line as a result of thermal excitation will not involve the crack line moving forward uniformly, which for an infinite long crack line would involve an infinite large energy barrier (as infinite many bonds would need to be broken at the same time), but small nano-sized regions will move nearly randomly in time. Therefore, the energy barrier for crack propagation discussed in the following corresponds to the barrier for the motion of a nano-sized crack-line segment.

Consider a crack propagating with a constant speed v in an infinite viscoelastic solid (see Fig. 6). The adhesive (or cohesive) bonds on the surface $z = 0$ in front of a crack tip can break before the stress from the crack reach the critical value σ_c, where the stress alone would break the bonds. This is due to thermal fluctuations, which can supply part of the energy needed to break a bond. Thermal effects are particularly important for weak bonds, e.g., van der Waals bonds.

We will denote a bond in front of the crack tip to be broken by the propagating crack as an interfacial bond. Let $P(t)$ be the probability that an interfacial bond is not broken at time t. We assume that the stress singularity in the continuum mechanics formalism occurs at a distance a behind the opening crack tip so the stress at the crack tip is finite. Let $x = vt$ (with $t \le 0$) be the position of the crack tip defined so that the stress on the surface $z = 0$ for $x > vt$ is given to leading order by

$$\sigma_{zz} = \frac{K_I}{2\pi(x + a - vt)^{1/2}}, \tag{8}$$

where K_I is the stress intensity factor for opening crack propagation. We denote $\sigma_{zz} = \sigma(t)$ for simplicity. In (8), we have assumed that the crack line is strait.

Now, consider an interfacial bond Q and choose the origin of the x axis so that the interfacial bond Q (broken or not broken) occupies the position $x = 0$ at $t = 0$. Let F_c denote the force to break the bond at zero temperature. For $T > 0$, the bond will break before the external force reaches F_c. This is due to thermal fluctuations, which can supply the energy needed to break a bond before the external force reaches the critical value F_c.

We consider the case where a broken bond can reform again. This will almost always be the case for weak bonds, such as the van der Waals bonds often involved in rubber adhering to a rigid substrate. In this case, a polymer chain at the interface can be in a state A,

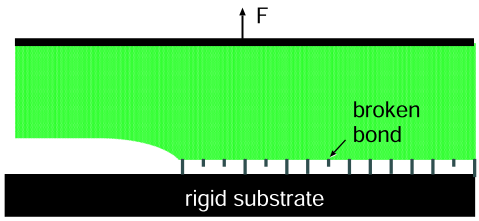

FIG. 6. For adhesive crack propagation, a fraction of the bonds will be broken by thermal fluctuations even far in front of the crack tip. The concentration of broken bonds increases as the crack tip is approached from the bonded side.

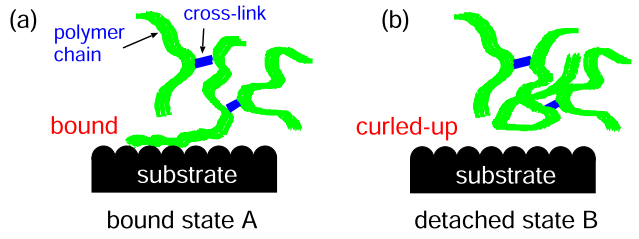

FIG. 7. Polymer chain in a bound state (a) and in the detached state (b). In the detached state, the chain is "curled-up" and an activation barrier of V_{form} must be overcome to form a new bonded state. The barrier V_{break} to break the bond is larger than V_{form}, and the chain spends most of the time in the bound state.

where it binds to the substrate or in a detached (curled-up) state B, as shown in Fig. 7. In the weakly stretched state far in front of the crack tip, an interfacial polymer chain is in the bound state A most of the time, but sometimes in a detached state B. We assume the potential energy has local minima for the bound state and for the detached state (see Fig. 8). The probability that the chain is in the bound state is denoted by P_A and in the detached state with P_B. We assume that $P_A(t)$ and $P_B(t)$ obey the rate equation,

$$\frac{dP_A}{dt} = -\kappa_A P_A + \kappa_B P_B, \tag{9}$$

where $P_A + P_B = 1$ is time-independent. We assume that

$$\kappa_A = \nu_A e^{-\beta V_{break}}, \qquad \kappa_B = \nu_B e^{-\beta V_{form}}, \tag{10}$$

where the barrier heights V_{break} and V_{form} are shown in Fig. 8 and depends on time due to the external force $F(t)$ stretching the chain. We assume (see Refs. 29–32) that $\nu_A = \nu_B = k_B T/h$, where h is the Planck constant. This is the Eyring expression for pre-exponential factors ν_A and ν_B.

Consider an interfacial bond Q as the crack tip approaches it. The local stress at bond Q is given by (8). We assume that the potential energy of a bond is given by

$$V(u) = V_A(u) + V_B(u), \tag{11}$$

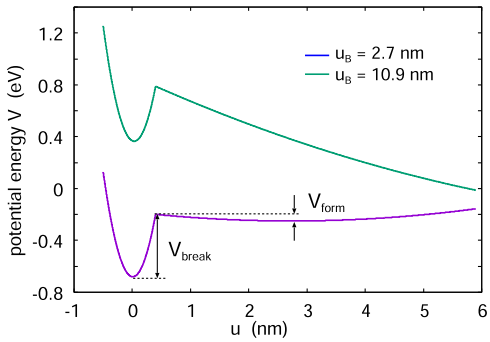

FIG. 8. Potential energy $V(u)$ [given by (11)–(13)] when the surface separation $u_B = 2.7$ and 10.9 nm. For $u_B = 10.9$ nm, the potential well of the detached state occurs for larger u than shown in the figure. For the parameters $U_{A0} = 0.5$ eV, $U_B = 0.25$ eV, $u_c = 0.4$ nm, $k_B = 0.003$ N/m, and $k_A = 2U_A/u_c^2 = 1.0$ N/m.

where

$$V_A(u) = -U_A + \frac{1}{2}k_A u^2 \tag{12}$$

for $u < u_c$ and $V_A(u) = 0$ for $u > u_c$, which correspond to a broken molecule–substrate bond, and

$$V_B = -U_B + \frac{1}{2}k_B(u - u_B)^2, \tag{13}$$

which is the energy of a stretched polymer chain. The polymer chain does not break so this is the energy of the chain for all chain (extension) length u.

The adiabatic work to break a bond is the difference in the potential energy after and before breaking the bond. The potential energy at the equilibrium state (with $u = u_B = 0$) is $-U_A - U_B$ and for the state with broken bond, $-U_B$. Therefore, the (adiabatic) work of adhesion $w_0 = U_B/b^2$ [which equals $G(v \to 0)$], where b^2 is the area occupied by the bonding segment of the polymer chain.

The chain–substrate bond breaks when

$$u = u_c = \left(\frac{2U_A}{k_A}\right)^{1/2}, \tag{14}$$

where the potential energy $V = V_1$ with

$$V_1 = V_B(u_c) = -U_B + \frac{1}{2}k_B(u_c - u_B)^2. \tag{15}$$

Before the bond is broken, the potential energy $V(u)$ is minimal when $V'(u) = 0$ or

$$k_A u + k_B(u - u_B) = 0$$

or

$$k_A u = K u_B, \tag{16}$$

where

$$K = \frac{k_A k_B}{k_A + k_B}. \tag{17}$$

Using (12), (13), and (16) in (11) gives the potential energy $V = V_0$ with

$$V_0 = -(U_A + U_B) + \frac{1}{2}K u_B^2. \tag{18}$$

Thus, the effective barrier for bond breaking is

$$\begin{aligned} V_{break} = V_1 - V_0 &= U_A + \frac{1}{2}k_B(u_c - u_B)^2 - \frac{1}{2}K u_B^2 \\ &= U_A + \frac{1}{2}k_B\left(u_c^2 - 2u_c u_B + \frac{k_B}{k_A + k_B}u_B^2\right). \end{aligned} \tag{19}$$

The energy barrier to form a bond when the surface separation equals u_B is

$$V_{form} = V_1 - [-U_B] = \frac{1}{2}k_B(u_c - u_B)^2. \tag{20}$$

It should be noted that when $k_B = 0$, then $V_{break} = U_A$ and $V_{form} = 0$ as expected.

If an external force F stretches the bond, then

$$k_A u = k_B(u_B - u) = F,$$

so the displacement $u = u_F = F/k_A$ and

$$u_B = \frac{F}{K}. \tag{21}$$

We denote the force to break the bond at zero temperature by $F_c = k_A u_c$. The displacement $u_B = u_{Bc}$ when the bond breaks (at zero temperature) is $u_{Bc} = F_c/K$, which we can also write as

$$u_{Bc} = \frac{k_A + k_B}{k_B} u_c.$$

Substituting $u_B = F/K$ in (19) and (20) gives the barriers $V_{break}(F)$ and $V_{form}(F)$ as a function of the applied force F.

Using $P_B = 1 - P_A$ from (9), we get

$$\frac{dP_A}{dt} = -\kappa P_A + \kappa_1, \tag{22}$$

where $\kappa = \kappa_A + \kappa_B$ and $\kappa_1 = \kappa_B$. In what follows, we denote $P_A = P$ for simplicity. Far at front of the crack tip, $dP/dt = 0$ so that $P = P_0$, where

$$P_0 = \frac{\kappa_1}{\kappa} = \frac{1}{1 + e^{-\beta \Delta E_0}},$$

where $\Delta E_0 = V_{break} - V_{form}$ is the energy difference between the two potential wells.

From (21), we get

$$P(t) = P(-\infty) \exp\left(-\int_{-\infty}^{t} dt' \kappa(t')\right) + \int_{-\infty}^{t} dt' \kappa_1(t') \exp\left(-\int_{t'}^{t} dt'' \kappa(t'')\right). \tag{23}$$

VI. DEPENDENCE OF THE CRACK ENERGY ON CRACK-TIP SPEED AND TEMPERATURE

Now, consider a molecular bond at $x = 0$ as the crack tip approaches it from far away ($t < 0$). A bond experiences the force,

$$F(t) = \frac{K_I b^2}{2\pi(a - vt)^{1/2}},$$

as the crack tip approaches it. We choose a so that $F(0) = F_c$, so that

$$F(t) = F_c\left(\frac{a}{a - vt}\right)^{1/2}, \tag{24}$$

where

$$F_c = \frac{K_I b^2}{2\pi\sqrt{a}}. \tag{25}$$

We assume plain stress state, and for this case, the crack-energy G is related to K_I using[33,34]

$$G = \frac{K_I^2}{E}, \tag{26}$$

which gives

$$G = \left(\frac{F_c 2\pi}{b^2}\right)^2 \frac{a}{E}. \tag{27}$$

The crack energy as $v \to 0$ is given by

$$G_{00} \approx \frac{U_A}{b^2} = \frac{1}{2b^2} k_A u_c^2 = \frac{1}{2b^2 k_A} F_c^2, \tag{28}$$

so we can write

$$G = \frac{a}{a_0} G_{00}, \tag{29}$$

where

$$a_0 = \frac{b^2 E}{8\pi^2 k_A}. \tag{30}$$

The work per unit area to propagate the crack is

$$G = \frac{1}{b^2} \int_{-\infty}^{0} dt\ u_B(t) F(t) P(t).$$

Changing the integration variable to $x = a - vt$ gives

$$G = \frac{1}{b^2} \int_a^{\infty} dx \left[-\frac{du_B}{dx}\right] F(x) P(x) \tag{31}$$

and from (23) with $dt = -dx/v$,

$$P(x) = P(\infty) \exp\left(-\frac{1}{v}\int_x^{\infty} dx' \kappa(x')\right) + \frac{1}{v}\int_x^{\infty} dx' \kappa_1(x') \exp\left(-\frac{1}{v}\int_x^{x'} dx'' \kappa(x'')\right). \tag{32}$$

For any finite x, the first integral in (32) will vanish because $\kappa(x)$ approaches a constant finite value for large x. Hence, we get

$$P(x) = \frac{1}{v}\int_x^{\infty} dx' \kappa_1(x') \exp\left(-\frac{1}{v}\int_x^{x'} dx'' \kappa(x'')\right). \tag{33}$$

From (24),

$$F = F_c\left(\frac{a}{x}\right)^{1/2} \tag{34}$$

and using that, $F = K u_B$ gives

$$-\frac{du_B}{dx} = -\frac{1}{K}\frac{dF}{dx} = \frac{F_c}{2K}\frac{a^{1/2}}{x^{3/2}}.$$

Thus, (31) becomes

$$G = \frac{F_c^2}{2Kb^2} \int_a^{\infty} dx\ \frac{a}{x^2} P(x). \tag{35}$$

At zero temperature, $P(x) = 1$ for $x > 0$ so that the crack propagation energy $G = G_1$ for $T = 0$ is

$$G_1 = \frac{F_c^2}{2Kb^2} \int_a^{\infty} dx\ \frac{a}{x^2} = \frac{F_c^2}{2Kb^2}. \tag{36}$$

Using that $Ku_{Bc} = F_c$, the r.h.s of (36) can also be written as $F_c u_{Bc}/2b^2$. Using (35) and (36), we get

$$\frac{G}{G_1} = \int_a^\infty dx\, \frac{a}{x^2} P(x). \tag{37}$$

Let us consider the limits $v \to 0$ and $v \to \infty$. As $v \to \infty$, the integrals in (33) will be dominated by the large x' and x'' regions and we can replace $\kappa_1(x')$ and $\kappa(x'')$ with their values for large x, which we denote by κ_{1eq} and κ_{eq}, since these are the thermal equilibrium rate constants. We get

$$P(x) \approx \frac{1}{v}\kappa_{1eq}\int_x^\infty dx' \exp\left(-\frac{1}{v}\kappa_{eq}(x'-x)\right) = \frac{\kappa_{1eq}}{\kappa_{eq}}, \tag{38}$$

which is equal to the probability $P_{eq} = \kappa_{1eq}/\kappa_{eq}$ that an interfacial molecule is in the binding state A far at front of the crack tip. Using (37), we get $G \to G_\infty$ as $v \to \infty$, where

$$\frac{G_\infty}{G_1} = \int_a^\infty dx\, \frac{a}{x^2}\frac{\kappa_{1eq}}{\kappa_{eq}} = \frac{\kappa_{1eq}}{\kappa_{eq}} = P_{eq}.$$

In the numerical study presented in the following, $P_{eq} \approx 1$, and hence, $G = G_1 P_{eq} \approx G_1$ as $v \to \infty$. However, in general for weak bonds and high temperatures $P_{eq} < 1$ and $G < G_1$ so high crack-tip speed is not always equivalent to low temperatures.

Next, consider the limit $v \to 0$. In that case, only a small $[x' - x]$ interval will contribute to the inner integral in (33) and we can replace $\kappa(x'')$ with its value for $x'' = x$. This gives

$$P(x) \approx \frac{1}{v}\int_x^\infty dx' \kappa_1(x') \exp\left(-\frac{1}{v}\kappa(x)(x'-x)\right).$$

For $v \to 0$, only x' that is very close to x will contribute to this integral, and we can replace $\kappa_1(x')$ with $\kappa_1(x)$ to get

$$P(x) \approx \frac{\kappa_1(x)}{\kappa(x)}.$$

Using this in (37), we get $G \to G_{00}$ as $v \to 0$, where

$$\frac{G_{00}}{G_1} = \int_a^\infty dx\, \frac{a}{x^2}\frac{\kappa_1(x)}{\kappa(x)}.$$

Writing $\xi = a/x$, this gives

$$\frac{G_{00}}{G_1} = \int_0^1 d\xi\, \frac{\kappa_1(\xi)}{\kappa(\xi)}.$$

Changing integration variable in (37) and (32) from x to $\xi = a/x$ gives

$$\frac{G}{G_1} = \int_0^1 d\xi\, P(\xi) \tag{39}$$

and

$$P(\xi) = \frac{a}{v}\int_0^\xi d\xi'\, \frac{\kappa_1(\xi')}{[\xi']^2} \exp\left(-\frac{a}{v}\int_{\xi'}^\xi d\xi''\, \frac{\kappa(\xi'')}{[\xi'']^2}\right). \tag{40}$$

Since κ and κ_1 are functions of u_B, we need to relate u_B to $\xi = a/x$. Using (34), we get

$$u_B = \frac{F}{K} = \frac{F_c}{K}\left(\frac{a}{x}\right)^{1/2} = \frac{F_c}{K}\xi^{1/2}.$$

For numerical calculations, the ξ'' integral in (40) is problematic as $v \to 0$, where only a very small $\xi - \xi'$ interval will effectively contribute. This problem is solved by using η as integration variable instead of ξ''; the variable η is defined by $\xi'' = \xi e^{-\eta}$, giving $d\xi'' = -\xi'' d\eta$ and

$$\int_{\xi'}^\xi d\xi''\, \frac{\kappa(\xi'')}{[\xi'']^2} = \int_0^{\eta_0} d\eta\, \frac{\kappa(\xi'')}{\xi''},$$

where $\eta_0 = \log(\xi/\xi')$.

A. Numerical results and discussion

The theory for $G(v, T)$ presented above depends on a set of parameters, the most important being U_A, k_B, and the temperature T. Here, we will present numerical results illustrating this. The reference case (green curves shown in Figs. 9 and 10) is obtained using $T_0 = 20\,^\circ$C, $U_A = 0.5$ eV, $U_B = 0.25$ eV, $k_B = 0.003$ N/m, and $u_c = 0.4$ nm.

Figure 9 shows the crack-energy G in units of its zero temperature value $G_1 = G(T = 0)$ as a function of the crack-tip speed (log–log scale) for the bond energies $U_A = 0.3$, 0.5, and 0.7 eV, and the other parameters as for the reference case. For $U_A = 0.3$, 0.5, and 0.7 eV, we have $G_1 b^2 = 60.4$, 167.4, and 327.8 eV, respectively.

Figure 10 shows similar results as shown in Fig. 9 for the temperatures $T = -30$, 20, and 70 °C, and Fig. 11 for the spring constants, $k_B = 0.001$, 0.003, and 0.006 N/m, and the other parameters as for the reference case. For $k_B = 0.001$, 0.003, and 0.006 N/m, we have $G_1 b^2 = 501.2$, 167.4, and 84.0 eV.

The numerical results in Figs. 9 and 10 show a low velocity range where $G_0(v)$ is velocity-independent, followed by a very abrupt increase in $G_0(v)$ at a characteristic speed v_c, which depends

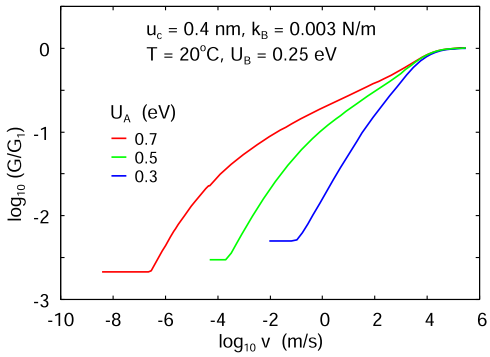

FIG. 9. Crack-energy G in units of its zero temperature value $G_1 = G(T = 0)$ as a function of the crack-tip speed (log-log scale) for the bond energies $U_A = 0.3$, 0.5, and 0.7 eV. For $T = 20\,^\circ$C, the spring constant $k_B = 0.003$ N/m, the separation to break the bond $u_c = 0.4$ nm, and the bond energy $U_B = 0.25$ eV is used. For the three cases with $U_A = 0.3$, 0.5, and 0.7 eV, we have $G_1 b^2 = 60.4$, 167.4, and 327.8 eV.

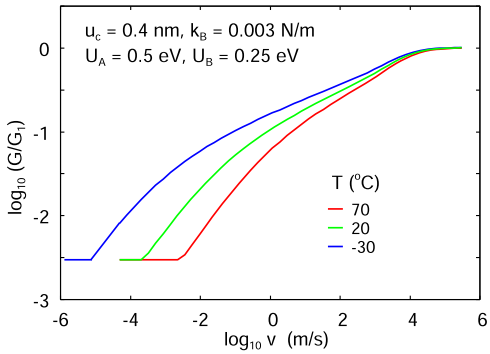

FIG. 10. Crack-energy G in units of its zero temperature value $G_1 = G(T = 0)$ as a function of the crack-tip speed (log–log scale) for the temperatures $T = -30$, 20, and 70 °C. The spring constant $k_B = 0.003$. For the A-well bond energy $U_A = 0.5$ eV, the separation to break the bond is $u_c = 0.4$ nm, and the B-well bond energy is $U_B = 0.25$ eV.

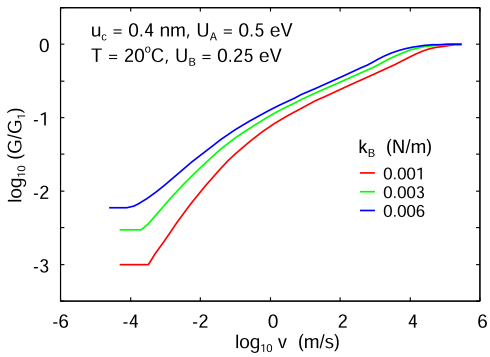

FIG. 11. Crack-energy G in units of its zero temperature value $G_1 = G(T = 0)$ as a function of the crack-tip speed (log–log scale) for the spring constants $k_B = 0.001$, 0.003, and 0.006 N/m. For $T = 20$ °C, the A-well bond energy is $U_A = 0.5$ eV, the separation to break the bond is $u_c = 0.4$ nm, and the B-well bond energy $U_B = 0.25$ eV. For the three cases with $k_B = 0.001$, 0.003, and 0.006 N/m, we have $G_1 b^2 = 501.2$, 167.4, and 84.0 eV.

on the binding energy U_A, the spring constant k_B, and the temperature T. In the low velocity "adiabatic" region where $v < v_c$, the separation of the surfaces at the crack tip is so slow that at any moment in time the molecules are in dynamical (kinetic) equilibrium between the bonding state A and the detached state B. That is, an interfacial molecule oscillates (randomly) during separation between the states A and B in such a way that the ratio of the probability to find the system in state B and A is given by the Boltzmann factor $\exp(-\beta\Delta E)$, where $\Delta E = V_{\text{break}} - V_{\text{form}}$ is the (separation dependent) energy difference between the two states. This is similar to the behavior of fluids at low shear rate.

Figure 9 shows that the critical velocity v_c decreases as the binding energy U_A increases. For binding energies as large as expected for cohesive cracks (~3 eV), v_c will be so low that no adiabatic velocity region can be observed on any time scale involving human activities (see Sec. VIII). Nevertheless, $G_0(v)$ will depend on the velocity, and only for relative high velocities will $G_0(v)$ be velocity independent. The reason is that independent of the magnitude of U_A when the external force has pulled the bond close to the point where the bond would be broken by the applied force alone, the remaining barrier for bond breaking will be overcome by a thermal fluctuation resulting in a velocity-dependent $G_0(v)$. This is also clear from Fig. 9 where for all the studied cases, $G_0(v)$ reach the high-velocity plateau for $\sim 10^4$ m/s.

Figure 11 shows that variations in the spring constant k_B result in relatively small variations in the critical velocity v_c. However, the magnitude of the ratio between the high-velocity $G_0(v)$ and of $G_0(v)$ in the adiabatic velocity region increases strongly with decreasing k_B. This is expected from the Lake and Thomas description of the dependency of the crack energy on the chain length (between cross links); decreasing k_B correspond to increasing chain length L ($k_B \sim 1/L$).

Figure 10 shows that as the temperature decreases, v_c decreases. This is a trivial result because thermal fluctuations decrease with decreasing temperature, and for $T \to 0$, we have $G \to G_1$ and $v_c \to 0$.

The abrupt increase in $G_0(v)$ at $v = v_c$ shown in Figs. 9–11 is in good agreement with what we have found in adhesion experiments for PDMS in contact with glass surfaces, as shown in Fig. 1. Using a reasonable binding energy $U_A = 0.5$ eV (see Sec. I) and a reasonable spring constant of order 0.003–0.006, we get the onset of non-adiabatic effects at a critical velocity $v_c \approx 0.1$ mm s^{-1}, in good agreement with the experiments (see Fig. 1). Furthermore, in the velocity region studies, $G_0(v)$ increases nearly linearly with v on the log–log scale, both in the experiment and in theory. This indicates $G_0 \sim v^{\alpha}$ with $\alpha \approx 0.22$ in the experiment (Fig. 1 and Ref. 35). The theory predicts a somewhat larger α (about 0.53 and 0.33 for $k_B = 0.003$ and $k_B = 0.006$, respectively) but this may reflect the simplicity of the model used or other complications. Thus, the experimental results in Ref. 38 for the same system but with different cross-link densities gave a similar critical velocity v_c, as shown in Fig. 12, but larger α exponents (0.34 and 0.5 for 1:30 and 1:20 cross-linker/base; for the 1:10 cross-linker/base too few data points were measured to determine an accurate α, but the obtained results indicate an exponent even larger than for the 1:20 case). The reason for the spread in the experimentally obtained values for the exponent α is not clear.

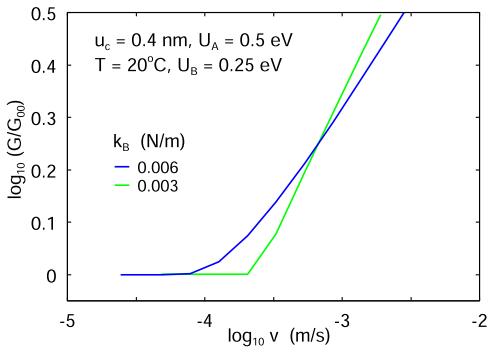

FIG. 12. Crack-energy G in units of its low-velocity value $G_{00} = G(v = 0)$ as a function of the crack-tip speed (log–log scale) for the spring constants $k_B = 0.001$ and 0.006 N/m. For $T = 20$ °C, the A-well bond energy is $U_A = 0.5$ eV, the separation to break the bond is $u_c = 0.4$ nm, and the B-well bond energy $U_B = 0.25$ eV. For the two cases with $k_B = 0.001$ and 0.006 N/m, we have $G_1 b^2 = 501.2$ and 84.0 eV.

VII. DEPENDENCY OF THE WORK OF ADHESION ON THE SEPARATION SPEED AND THE TEMPERATURE

The breaking of adhesive bonds between two solids usually occur by interfacial crack propagation. However, for very small contact regions, the bond may break uniformly (simultaneously) over the contact region.[39] In any case, the work of adhesion w is usually defined as the work to separate two flat solid surfaces with the surfaces parallel. In this section, we will consider the separation of two parallel surfaces where the separation speed is constant. It should be noted that this differs from interfacial crack propagation where the separation velocity depends on the distance from the crack tip.

Consider the simplest case of separating the surfaces uniformly at the speed v from the equilibrium position. In this case, $u_B(t) = v_z t$, where we have used that the total energy is minimal for $u_B = 0$. Using (21), the external force,

$$F(t) = Kv_z t.$$

The force to separate the surfaces per unit surface area is $F(t)P(t)/b^2$ and the work per unit surface area w to separate the surfaces,

$$w = \frac{1}{b^2}\int_0^{t_0} dt\, v_z F(t) P(t),$$

where $v_z t_0 = u_{Bc}$. If we introduce $\xi = v_z t/u_{Bc}$, we get

$$w = \frac{K u_{Bc}^2}{b^2}\int_0^1 d\xi\ \xi P(\xi).$$

In the limiting case of zero temperature, $P(t) = 1$ for $t < t_0$ or $\xi < 1$ so that the work of adhesion w_1 at zero temperature,

$$w_1 = \frac{K u_{Bc}^2}{b^2}\int_0^1 d\xi\ \xi = \frac{K u_{Bc}^2}{2b^2},$$

which also equals $u_{Bc}F_c/2b^2$. Hence,

$$\frac{w}{w_1} = 2\int_0^1 d\xi\ \xi P(\xi). \tag{41}$$

Using $\xi = v_z t/u_{Bc}$, we also get

$$P(\xi) = P(0)\exp\left(-\frac{u_{Bc}}{v_z}\int_0^\xi d\xi'\kappa(\xi')\right) + \frac{u_{Bc}}{v_z}\int_0^\xi d\xi'\kappa_1(\xi')\exp\left(-\frac{u_{Bc}}{v_z}\int_{\xi'}^\xi d\xi''\kappa(\xi'')\right). \tag{42}$$

The rate coefficients $\kappa_1(\xi)$ and $\kappa(\xi)$ are functions of u_B but can be considered as functions of ξ by replacing $u_B = \xi u_{Bc}$.

One interesting limit of this equation is $v \to 0$, where (42) reduces to $P = P_0 = \kappa_1(\xi)/\kappa(\xi)$. This limit also follows directly from the rate Eq. (22) when $dP/dt = 0$ and corresponds to the assumption that thermal equilibrium occur at all stages in the pull-off. Using $P = P_0$ in (41) gives $w \approx U_0/b^2$, i.e., the adiabatic work of adhesion.

For numerical calculations, the ξ'' integral in (42) is problematic as $v \to 0$, where only a very small $\xi - \xi'$ interval will effectively contribute. This problem is solved by using η as integration variable instead of ξ''; the variable η is defined by $\xi'' = \xi e^{-\eta}$, giving $d\xi'' = -\xi'' d\eta$ and

$$\int_{\xi'}^{\xi} d\xi''\kappa(\xi'') = \int_0^{\eta_0} d\eta\,\xi''\kappa(\xi''),$$

where $\eta_0 = \log(\xi/\xi')$.

A. Numerical results and discussion

Figures 13–15 show the work of adhesion w in units of its zero temperature value $w_1 = w(T = 0)$ as a function of the pull-off speed (log-log scale) for different bond energies (Fig. 13), different temperatures (Fig. 14), and different spring constants k_B (Fig. 15). For $U_A = 0.3$, 0.5, and 0.7 eV, we have $\mathcal{E}_1 = w_1 b^2 = 60.4$, 167.4, and 327.8 eV. The dashed lines in the figures shows the crack-energy $G(v)/G_1$ as a function of the crack-tip speed (log–log scale, from Figs. 9 and 10) using the same parameters as used for the same colored solid lines. The work of adhesion curves shows a similar dependence on the pull-off speed as the crack energy on the crack-tip speed, but are shifted along the velocity axis as expected because the crack-tip speed (in the x-direction) is not the same as the crack opening speed (in the z-direction), and the latter depends on time even when the crack-tip speed is constant.

It is important to note the following fact: for $T > 0$ K, an arbitrary small force can break an adhesive bond and remove a molecule from a surface. If the bond is strong or the temperature low, a very long time will be needed for a large enough thermal fluctuation to occur to break the bond. Nevertheless, even without an applied force, a molecule will desorb from a surface after a long enough time. However, for molecules binding two nominally flat and infinite large surfaces, the situation is different. In this case, even if the bonds are very weak, a small applied pull-pressure cannot separate the surfaces. The reason is that even if each individual molecule fluctuates between the bonded and non-bonded state, a non-zero fraction of the molecules will be in the bonded state. That is, if thermodynamic

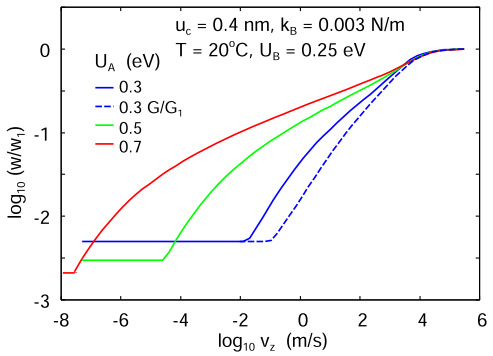

FIG. 13. Work of adhesion w in units of its zero temperature value $w_1 = w(T = 0)$ as a function of the pull-off speed (log–log scale) for the bond energies $U_A = 0.3$, 0.5, and 0.7 eV. For the temperature $T = 20$ °C and the spring constant $k_B = 0.003$ N/m, the separation to break the bond is $u_c = 0.4$ nm and the bond energy is $U_B = 0.25$ eV. For the three cases with $U_A = 0.3$, 0.5, and 0.7 eV, we have $\mathcal{E}_1 = w_1 b^2 = 60.4$, 167.4, and 327.8 eV.

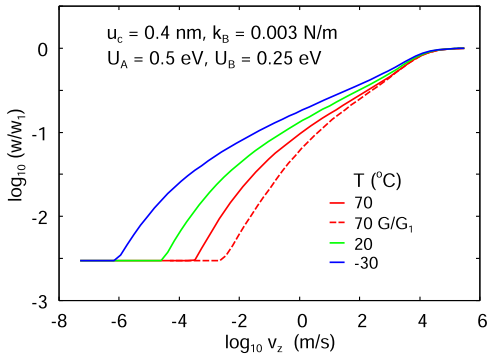

FIG. 14. Work of adhesion w in units of its zero temperature value $w_1 = w(T = 0)$ as a function of the pull-off speed (log–log scale) for the temperatures $T = -30$, 20, and 70 °C The spring constant is $k_B = 0.003$. For the A-well bond energy $U_A = 0.5$ eV, the separation to break the bond is $u_c = 0.4$ nm, and the B-well bond energy is $U_B = 0.25$ eV.

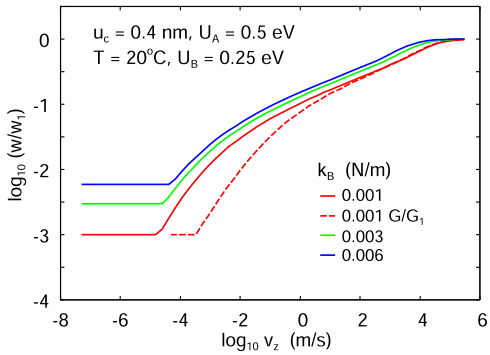

FIG. 15. Work of adhesion w in units of its zero temperature value $w_1 = w(T = 0)$ as a function of the pull-off speed (log–log scale) for the spring constants $k_B = 0.001$, 0.003, and 0.006 N/m. For $T = 20$ °C, the A-well bond energy $U_A = 0.5$ eV, the separation to break the bond is $u_c = 0.4$ nm, and the B-well bond energy is $U_B = 0.25$ eV. For the three cases with $k_B = 0.001$, 0.003, and 0.006 N/m, we have $\mathcal{E}_1 = w_1 b^2 = 501.2$, 167.4, and 84.0 eV.

(or kinetic) equilibrium occurs, any given molecule will fluctuate (in time) between the two states but when considering a large number of molecules, a (constant) fraction of the molecules will be in the bonded state (see Fig. 16). For this case, the work to slowly remove the contact between the solids will equal to the thermodynamic work of adhesion, which is equal to the change in the free energy between the system with separated surfaces and the system in contact at the equilibrium separation.

VIII. COHESIVE CRACK PROPAGATION

The stress in the vicinity of cohesive cracks in rubber materials is so high that linear viscoelasticity is unlikely to be valid even several nm away from the crack tip. Depending on the material considered, one may need to take into account non-linear elasticity, plastic deformation, or the formation of defects, such as cavities or stringing, in a region close to the crack tip. Most of these processes are

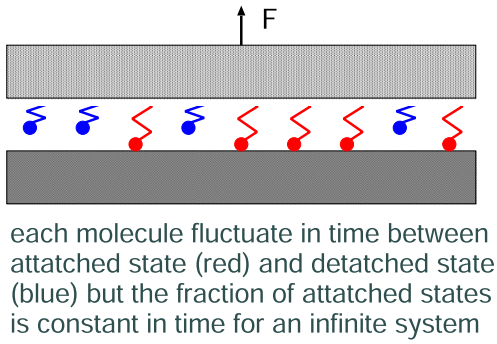

FIG. 16. If thermodynamic (kinetic) equilibrium occurs, any given molecule will fluctuate (in time) between the bonding and non-bonding states, but when considering a large number of molecules, a non-zero fraction of the molecules will be in the bonding state.

strongly temperature-dependent and will contribute via the factor $G_0(v, T)$ to the crack energy.

It has recently been suggested[53–55] that the (v, T) dependency of the dissipation in the crack-tip process zone may be more important for the crack energy than the viscoelastic factor $[1 + f(T, v)]$. This may indeed be the case for conditions, where the viscoelastic effect is very small, such as for temperatures much higher than the rubber glass transition temperature. However, in general, the viscoelastic factor is extremely important and increases by a factor of E_∞/E_0 (where E_∞ and E_0 are the high and low frequency modulus, respectively) between high and low sliding speeds (or low and high temperatures). For most rubber compounds $E_\infty/E_0 \sim 10^3$, and for weakly crosslinked rubber even more.

Here, we present numerical results illustrating the velocity dependency of $G_0(v, T)$ for cohesive cracks, resulting from stress aided thermally activated bond-breaking. We use the same model as in Sec. VI, but the meaning of the U_A, U_B, u_c, k_A, and k_B parameters differ. Thus, the spring constant k_B in Sec. VI was of entropic origin as relevant for breaking of weak adhesive bonds. For breaking cohesive bonds, the chains in the process zone will stretch so strongly that the entropic elasticity is irrelevant. In the theory of Lake and Thomas, it was assumed that just before a chain breaks at one of the (covalent) bonds, it is stretched so that all the bonds along the chain are close to the breaking point. Thus, the elastic energy stored in a chain consisting of N^* bond-units, at the point where a bond will break, is $N^* U_A$, where U_A is the energy to break a bond. (It should be noted that $N^* \gg N$ since the separation between the covalent bonds is ≈0.1 nm while the Kuhn length $b \approx 1$ nm.) In this case, the crack energy (neglecting thermal activation) is obtained by multiplying $N^* U_A$ with the number of chains per unit area crossing the fracture plane. Using this approach, Lake and Thomas estimated the fracture energy G_0 and found it to be typically of order 10 J/m^2 or 100 eV/nm^2, which is close to what is observed under conditions where the viscoelastic factor $[1 + f(v, T)]$ is small.

Figure 17 shows the crack-energy G in units of its zero temperature value $G_1 = G(T = 0)$ as a function of the crack-tip speed for $T = 20$ °C, under conditions typical for adhesive cracks (green line) and cohesive cracks (blue and red lines are for $U_A = 3$ and 1.5 eV, respectively). For the cohesive crack (blue line), we have

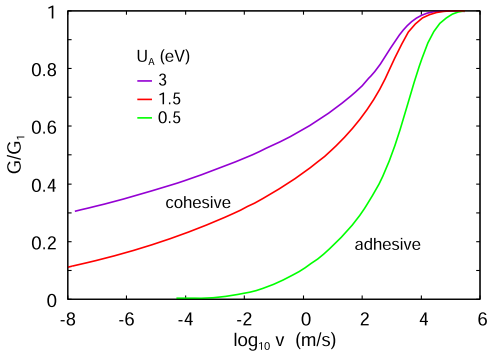

FIG. 17. Crack-energy G in units of its zero temperature value $G_1 = G(T = 0)$ as a function of the crack-tip speed for $T = 20\,^{\circ}\mathrm{C}$, under conditions typical for adhesive cracks (green line) and cohesive cracks (blue and red lines). In the calculations for adhesive crack, we used (green line) $U_A = 0.5$ eV, $U_B = 0.25$ eV, $k_B = 0.003$ N/m, $k_A = 2U_A/u_c^2 \approx 1.0$ N/m, and $u_c = 0.4$ nm, and for the cohesive cracks (blue line), $U_A = U_B = 3$ eV, $u_c = 0.1$ nm, $k_A = 2U_A/u_c^2 \approx 96.1$ N/m, and $k_B = k_A/N^*$ with $N^* = 30$, and (red line) $U_A = U_B = 1.5$ eV, $u_c = 0.1$ nm, $k_A = 2U_A/u_c^2 \approx 48.1$ N/m, and $k_B = k_A/N^*$ with $N^* = 30$.

used $U_A = U_B = 3$ eV, $u_c = 0.1$ nm, $k_A = 2U_A/u_c^2$, and $k_B = k_A/N^*$ with $N^* = 30$ giving $N^* U_A = 90$ eV. Because of the much higher energy needed to break a covalent bond in the chain compared to the adhesion bond, the variation of the crack energy with the crack-tip speed is much slower for the cohesive crack. For the adhesive crack, the thermal equilibrium crack energy is reached already for $v \approx 0.1$ mm s^{-1} (as also observed in experiments; see Fig. 1), but for the cohesive cracks, the thermal equilibrium value cannot be reached at any crack-tip velocity of human interest. We conclude that for cohesive cracks, the viscoelastic factor $[1 + f(v, T)]$ will, in general, result in a much stronger velocity dependence than that of the prefactor $G_0(v, T)$, at least for the bond-breaking process considered here.

Figure 18 shows the crack-energy G in units of its zero temperature value $G_1 = G(T = 0)$ as a function of the logarithm of the crack-tip speed for $U_A = 1.5$ eV for two different spring constants, $k_B = 1.6$ (red line) and 0.24 N/m (green line). The difference between the two cases for very small sliding speeds is very small but this is the case only for the ratio G/G_1 since $G_1 \sim k_B^2$ differ by a factor of $(1.6/0.24)^2 \approx 44.4$.

In a beautiful experimental study, Chaudhury has measured the velocity dependency of the fracture energy for PDMS films chemically bound to silanized silica glass surfaces. Using an elegant experimental setup of the JKR-type, he was able to measure $G(v)$ at extremely small crack tip speeds, from 0.1 to 100 nm s^{-1}. For these low crack tip speeds, the used silicon rubber can be considered as a perfect elastic material so the crack energy is determined by the prefactor $G_0(v, T)$ in Eq. (1). Using a simple picture of the bond breaking at the crack tip, assuming that the bond-breaking occurs with a constant separation velocity, he showed that for low separation velocities v_z, the energy $\mathcal{E}$ to break a bond $\mathcal{E}^{1/2} \sim \ln v_z$. I have not been able to derive this result analytically using the theory for $G(v)$ presented above, but the numerical results that we now present indicate that $G^{1/2} \sim \ln v$ holds reasonably well for low crack tip speeds.

Figure 19 shows the relation between $G^{1/2}$ and $\ln v$ for the system studied by Chaudhury. The squares represent the measured data from Ref. 52 and the solid line represents the theory prediction. The calculation used (39) and (40) with $G_1 = cN^* U_A$, $U_A = 1.5$ eV, and $N^* = 208$, corresponding to the spring constant $k_B = 0.245$ N/m. The number density of polymer chains crossing the fracture plane was estimated by Chaudhury, using the method of Lake and Thomas, and was found to be $c = 2.5 \times 10^{18}$ m^{-2} (also see Appendix B). This gives $G_1 = G_0(T = 0) = 128$ J/m^2. The beautiful agreement between the theory and the experiment should be noted. Chaudhury argued that the energy to break one bond ($U_A = 1.5$ eV) is due to siloxane bond scission, which is close to that (1.5–1.8 eV) obtained from thermal de-polymerization and stress relaxation kinetics of the siloxane polymers.

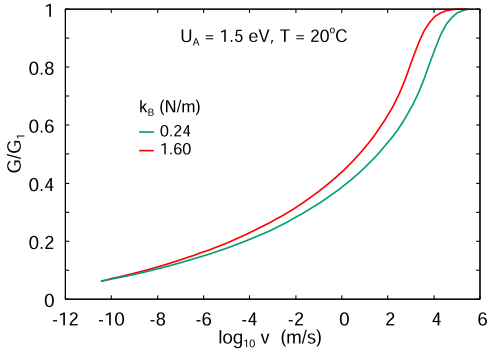

FIG. 18. Crack-energy G in units of its zero temperature value $G_1 = G(T = 0)$ as a function of the crack-tip speed for $T = 20\,^{\circ}\mathrm{C}$, under conditions typical for cohesive cracks. In the calculations for adhesive crack, we used (red line) $U_A = U_B = 1.5$ eV, $u_c = 0.1$ nm, $k_A = 2U_A/u_c^2 \approx 48.1$ N/m, and $k_B = k_A/N^*$ with $N^* = 30$, and (green line) for the same parameters except with $N^* = 30$ replaced by $N^* = 200$.

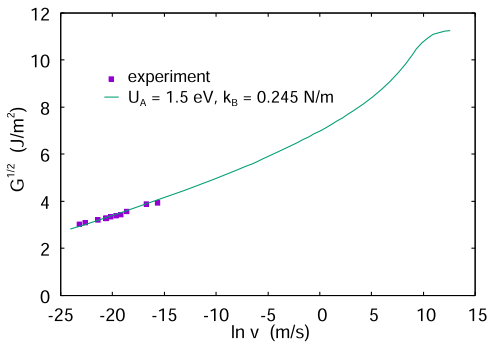

FIG. 19. Square-root $G^{1/2}$ of the crack energy as a function of the (natural) logarithm $\ln v$ of the crack-tip speed for $T = 20\,^{\circ}\mathrm{C}$. The squares represent the measured data from Ref. 52 and the solid line represents the theory prediction. In the calculation, we used $U_A = U_B = 1.5$ eV, $u_c = 0.1$ nm, $k_A = 2U_A/u_c^2 \approx 48.1$ N/m, and $k_B = 0.245$ N/m.

IX. DISCUSSION

For non-zero temperature, crack propagation is possible in all solids if the elastic energy released is larger than the critical crack-energy G_{00} determined by the change in the (thermal equilibrium) free energy upon formation of the crack surfaces. However, in solids with strong bonds, the crack will propagate with extremely low velocities (creep) if G is close to G_{00}, as shown in Fig. 17 for polymers and in Ref. 65 for silicone. In the latter case, crack's moves by the formation and propagation of kinks involving breaking of single atomic bonds at the crack tip, which require relative small energy (~0.3 – 0.4 eV).[65]

In the absence of stress corrosion for zero temperature in elastic crystalline solids, such as silicon, crack's cannot propagate in a steady state for crack-tip velocities below some critical value v_c, which is of the order of the Rayleigh surface wave speed.[66] In addition, lattice pinning and hysteresis effects occur in such solids. This differs from cracks in viscoelastic solids, which can propagate at arbitrary low speed even when thermal bond-breaking effects at the crack-tip are unimportant, but where the bulk is viscoelastic (which require non-zero temperatures).[15,17] Nevertheless, no opening crack propagation is possible if the elastic energy released is smaller than the critical crack-energy G_{00}.

In the study in Secs. VI and VII, we have treated k_B as an entropic spring, which can be estimated using $k_B \approx Eb$, where E is the elastic modulus and $b \sim 1$ nm (see the Appendix A). For rubber-like materials, this is a good approximation for high enough temperature or low enough deformation rates, where the rubber is in the so called "rubbery" region. However, the viscoelastic modulus $E(\omega, T)$ of rubber increases strongly as the deformation frequency ω increases and may be 10^3 (or more) higher in the high frequency "glassy" region. This effect must be taken into account in a more general theory for $G_0(v, T)$ even if developed on the same simple level as in the present study. This generalization can be done in a similar way as described in Ref. 67 for the frictional shear stress (see in the following).

For viscoelastic materials, there will be a contribution to the crack energy from viscoelastic energy dissipation in front of the crack tip as described by the factor $[1 + f(v, T)]$ in (1). This contribution also depends on the crack-tip cutoff length $a(v, T)$, and for this reason, as discussed in Appendix C, the factors $G_0(v, T)$ and $f(v, T)$ in (1) are not independent of each other, i.e., the crack-tip process zone contribution and the viscoelastic (bulk) contribution to $G(v, T)$ are not independent.

The picture underlying the theory for adhesive crack propagation presented above is similar to the picture of the adhesive contribution to sliding friction proposed by Schallamach[68] and shown in Fig. 20. During lateral motion of the rubber block, the chain attaches (a), stretches (b), detaches (c), relaxes, and reattaches to the surface to repeat the cycle. In reality, no "full" detachment in the vertical direction is expected, but only a rearrangement of molecule segments (in nanometer-sized domains) parallel to the surface from pinned (commensurate-like) domains to depinned (incommensurate-like) domains. The work of Schallamach was extended to more realistic conditions by Chernyak and Leonov[69] and by Persson and Volokitin.[67] In Ref. 67, the full frequency-dependent modulus $E(\omega, T)$ was used when calculating the frictional shear stress.

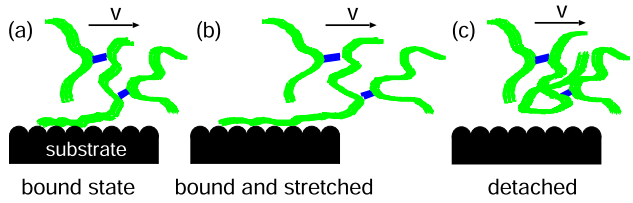

FIG. 20. Classical description of a polymer chain at the rubber-block countersurface interface. During lateral motion of the rubber block, the chain attaches (a), stretches (b), detaches (c), relaxes, and reattaches to the surface to repeat the cycle. The picture is schematic, and in reality, no detachment in the vertical direction is expected, but only a rearrangement of molecule segments (in nanometer-sized domains) parallel to the surface from pinned (commensurate-like) domains to depinned (incommensurate-like) domains.

Support for the importance of the bonding–stretching–debonding contribution to sliding friction was presented in Refs. 70 and 71 (see also Ref. 72), where it was shown that in addition to the viscoelastic deformations of the rubber surface by the road asperities, there is an important contribution to the rubber friction from shear processes in the area of contact. Analysis showed that the latter contribution could result from bonding–stretching–debonding cycles of the type shown in Fig. 20. However, temperature dependency of the shear stress τ_f, for temperatures above the rubber glass transition temperature T_g, was found to be weaker than that of the bulk viscoelastic modulus. The physical origin of this may relate to the rubber molecule segment mobility at the sliding interface, which for rough surfaces may be higher than in the bulk because of an increased free-volume effect due to the short-wavelength surface roughness. This is consistent with the often observed reduction in the glass transition temperature in nanometer-thick surface layers of glassy polymers. In Refs. 19 and 61, we argued that the opening crack propagation at the asperity contact regions, on very rough surfaces such as road surfaces, may not give an important contribution to the rubber friction in most cases.

X. SUMMARY AND CONCLUSION

In this paper, I have studied the influence of temperature and the crack-tip velocity of the bond breaking at the crack tip in rubber-like materials. The bond breaking is considered as a stress-aided thermally activated process, which results in an effective crack propagation energy, which increases with decreasing temperature or increasing crack-tip speed. The theory was developed for adhesive cracks (crack propagation between an elastic solid and a counter surface) but should also be valid for cohesive cracks if the only loss process is bond breaking at the crack tip as in the Lake and Thomas model of the crack tip process zone.

The model calculations show a very abrupt onset of non-adiabatic effects with increasing crack-tip speed. Thus, for $v < v_c$, where for a typical case of weak adhesion $v_c \sim 0.1$ mm s^{-1}, the bond-breaking occurs adiabatically, where the adhesion molecules fluctuate stochastically between the bonded and non-bonded state, as in thermal equilibrium (liquid-like) dynamics. For $v > v_c$, the crack-energy increases rapidly and may be ~10^3 bigger at high crack-

tip speed than in the adiabatic limit. These results are in reasonable agreement with the experimental data for silicone rubber bound to silica glass surfaces.

For cohesive cracks, the velocity dependency of $G_0(v,T)$ for $v > v_c$ is much weaker than for adhesive crack propagation, and the adiabatic limit ($v < v_c$) can never be reached on time or velocity scales involved in human activities. Hence, for cohesive cracks in rubber-like materials, the viscoelastic factor $[1 + f(v,T)]$ will almost always dominate the velocity (and temperature) dependency of the crack energy unless the experiments involve temperatures much higher than the rubber glass transition temperature or so low crack-tip speed that the rubber response is in the rubbery part of the viscoelastic spectra.

ACKNOWLEDGMENTS

I thank M. K. Chaudhury for useful discussions and for drawing my attention to his beautiful work in Ref. 52. I thank M. Ciavarella for discussions about the influence of thermal excitations on non-steady crack propagation. This work was supported by the Strategic Priority Research Program of the Chinese Academy of Science, Grant No. XDB0470200.

AUTHOR DECLARATIONS

Conflict of Interest

The author has no conflicts to disclose.

Author Contributions

B. N. J. Persson: Conceptualization (equal); Data curation (equal); Formal analysis (equal); Investigation (equal); Methodology (equal); Validation (equal); Writing – original draft (equal); Writing – review & editing (equal).

DATA AVAILABILITY

The data that support the findings of this study are available from the corresponding author upon reasonable request.

APPENDIX A: ESTIMATION OF THE SPRING CONSTANT k_B

In this section, we denote the spring constant k_B by k in order not to mix it up with the Boltzmann constant. There are different ways of estimating the spring constant k relevant for adhesive fracture. If a pressure p_0 is applied to a circular area of radius R on an elastic half space, it will displace the center of the surface with a distance $u = F/k$, where $F = \pi R^2 p_0$ is the applied force and the spring constant,

$$k = \beta R E, \tag{A1}$$

where β is of order unity [typically between 1 and 2 depending on the spatial variation of p_0, with $\beta = \pi/2(1-\nu^2)$ if p_0 is constant]. Using $R \approx 0.75$ nm and $E \approx 2$ MPa (as for fully cross-linked PDMS), we get $k \approx 0.003$ N/m.

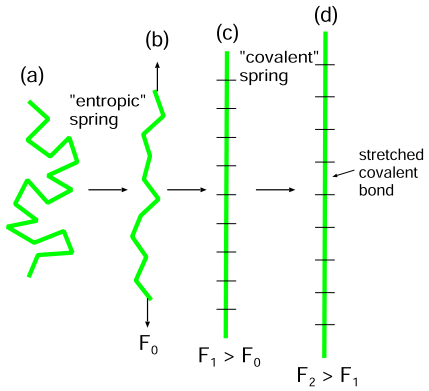

FIG. 21. Panel (a) and (b), adhesive fracture: a chain between a cross-link and a bond to a substrate. The chain stretches before the bond to the substrate breaks. The bond to the substrate is assumed weak and the relevant spring constant is the entropic spring constant. Panels (c) and (d), cohesive fracture: a chain between two crosslinks on the opposite sides of a fracture plane before the fracture. When the cross-links separate at a crack tip, the chain stretches before the chain break at any of the bonds along the chain. In this case, the separation force is so high that the relevant spring constant corresponds to stretching of the covalent bonds along the chain.

An alternative approach is to use the entropic spring constant [see Figs. 21(a) and 21(b)] of a chain of length L. Here, a "chain" denotes the part of a parent long-chain molecule lying between adjacent cross-links (see Fig. 2). A long-chain molecule acts as a spring in tension, with the restoring force based on changes in entropy rather than energy. This "entropic-spring" model has played a central role in the molecular theory of rubber elasticity. From the simplest "freely jointed chain model,"

$$k = \frac{3k_B T}{Lb}, \tag{A2}$$

where b is the length of a rigid (Kuhn) segment (monomer unit) and $L = Nb$, where N is the number of Kuhn segments in the chain. (Each Kuhn segment can be thought of as if they are freely jointed with each other. Each segment in a freely jointed chain can randomly orient in any direction without the influence of any forces, independent of the directions taken by other segments.) For Sylgard 1:10 PDMS, the Kuhn length $b \approx 1$ nm. Using $N = 4$ (or $L = Nb = 4$ nm) at room temperature, this gives $k \approx 0.003$ N/m.

Using Young's modulus predicted by the freely jointed chain model, one can show that the two expressions (A1) and (A2) are essentially equivalent. The Young's modulus,

$$E = \frac{3k_B T}{Ld^2}, \tag{A3}$$

where $d \approx 0.5$ nm is an effective diameter of the chain. Using this in (A1) gives

$$k = \frac{3\beta k_B T R}{Ld^2}, \tag{A4}$$

which equals (A2) if we choose $\beta R = d^2/b$. Since $b/d \approx 2$, this implies that the diameter of the circular surface region, where the applied

stress acts in the elastic continuum model in order to give the same spring constant as obtained from the entropic spring model, is of order of the effective diameter of the chain, which is what one would intuitively expect.

The spring constant estimated above is relevant for breaking weak adhesive bonds. For breaking cohesive bonds, the chains will stretch so strongly that the entropic elasticity is irrelevant [see Figs. 21(c) and 21(d)]. In the theory of Lake and Thomas, it is assumed that the chain to be broken is stretched so that each (chemical) bond along the chain is close to the point of breaking the bond. Thus, the energy stored in the chain with N^* chain bonds at the point where one bond break is $N^* U_A$, where $U_A \approx 3$ eV is the bond energy. If a chain is $L = 10$ nm and the distance between the bonds ~0.1 nm, we get $N^* = 100$ as a typical number for the number of chain bonds. In this case, the crack energy (neglecting thermal activation) is obtained by multiplying $N^* U_A$ with the number of chains per unit area crossing the fracture plane. Using this approach, Lake and Thomas estimated the fracture energy G_0 and found it to be typically of the order 10 J/m^2 or 100 eV/nm^2, which is close to the observed fracture energies for low crack-tip speeds.

APPENDIX B: ESTIMATION OF DENSITY OF THE CHAIN CROSSING THE FRACTURE PLANE

The fracture energy of polymers depends on the number of chains per unit area, c, crossing the fracture plane. Here, a "chain" denotes the part of a parent long-chain molecule lying between adjacent cross-links (see Fig. 2). Lake and Thomas[40] have estimated c, and here, for the readers' convenience, we give a slightly different derivation.

The maximum length of a chain is $L = Nb$, where N is the number of Kuhn segments. Assuming that the fracture plane is at $z = 0$. Any chain in the region $-L < z < L$ has some probability to extend across the fracture plane. If A is the surface area, the volume of the slab $-L < z < L$ is $V = 2AL$. If it contains n chain molecules, then $V = nLd^2$, where Ld^2 is the volume of a chain molecule of length L and effective (chain) diameter d. Using $V = 2AL = nLd^2$, the number of chains per unit surface area in the region $-L < z < L$ is $n/A = 2/d^2$ Of these chains, only a fraction p will cross the fracture plane. Thus, the concentration of chains crossing the fracture plane is

$$c = \frac{2p}{d^2}. \tag{B1}$$

For a Gaussian chain, the probability that it has the end-to-end length r is

$$P(r) = 4\pi r^2 \left(\frac{\alpha}{\pi}\right)^{3/2} e^{-\alpha r^2},$$

where

$$\alpha = \frac{3}{2Nb^2}. \tag{B2}$$

This probability distribution is normalized so that

$$\int_0^\infty dr\ P(r) = 1.$$

Of all chains of length r, only those at a distance $h < r$ from the fracture plane has a chance to cross the fracture plane. A chain of length r can have any angular orientation of the end-to-end vector so the probability that a chain of length r with one end point at a distance h from the fracture plane will cross the fracture plane is given by the area ratio $A(h)/A_0$, where $A_0 = 4\pi r^2$ and $A(h) = 2\pi rh$ (see Fig. 22). Thus, $A(h)/A_0 = h/2r$ and the probability that an arbitrary chosen chain will cross the surface $z = 0$ is

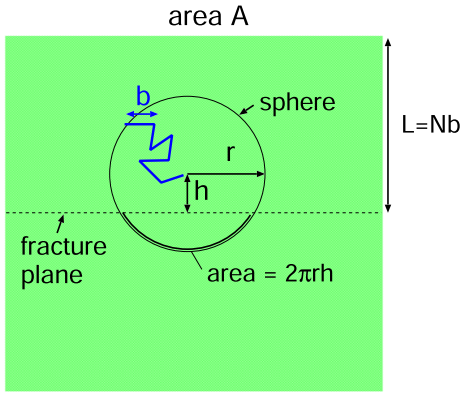

FIG. 22. Polymer with the end-to-end separation r and with one end point a distance h from the fracture plane has the probability $2\pi rh/4\pi r^2 = h/2r$ to cross the fracture plane.

$$p = \frac{1}{L}\int_0^L dh \int_0^\infty dr\ P(r)\theta(r-h)\frac{h}{2r} = \frac{1}{2L(\pi\alpha)^{1/2}}.$$

Using (B1) and (B2), this gives

$$c = \left(\frac{2}{3\pi}\right)^{1/2} \frac{1}{d^2\sqrt{N}}.$$

APPENDIX C: CRACK PROPAGATION INCLUDING THE VISCOELASTIC DISSIPATION CONTRIBUTION

For viscoelastic materials, there will be a contribution to the crack energy from viscoelastic energy dissipation in front of the crack tip, as described by the factor $[1 + f(v,T)]$ in (1). This contribution also depends on the crack tip cutoff length $a(v,T)$, and for this reason, the terms $G_0(v,T)$ and $[1 + f(v,T)]$ in (1) are not independent of each other.

In Ref. 17, it was shown that the crack energy, including the viscoelastic (bulk) contribution, is given by

$$G = G_0(v,T) + E_0 G \frac{2}{\pi}\int_0^1 d\xi \frac{1}{\xi}\left(1-\xi^2\right)^{1/2} \mathrm{Im}\frac{1}{E(2\pi\xi v/a)}$$

or

$$G = \frac{G_0(v,T)}{1 - E_0(2/\pi)\int_0^1 d\xi\ \xi^{-1}\left(1-\xi^2\right)^{1/2}\mathrm{Im}E^{-1}(2\pi\xi v/a)}, \tag{C1}$$

where $G_0(v,T)$ is given by (39) and (40),

$$G_0(v,T) = \frac{F_c^2}{2Kb^2}\int_0^1 d\xi\ P(\xi),$$

$$P(\xi) = \frac{a}{v}\int_0^{\xi} d\xi' \, \frac{\kappa_1(\xi')}{[\xi']^2} \exp\left(-\frac{a}{v}\int_{\xi'}^{\xi} d\xi'' \, \frac{\kappa(\xi'')}{[\xi'']^2}\right).$$

Equation (C1) together with (29),

$$G = \frac{a}{a_0} G_{00},$$

constitutes two equations for two unknown variables, G and a. It should be noted that since both the nominator and the denominator in (C1) depends on the cutoff length a, the process-zone factor $G_0(v,T)$ and viscoelastic factor $[1+f(v,T)]$ in (1) are not independent of each other as usually assumed.

In the limit $v \to \infty$, the denominator in (C1) becomes E_0/E_∞, where $E_\infty = E(\omega = \infty)$ is the high frequency modulus. This is easily proved by changing integration variable to $\omega = 2\pi\xi v/a$ and using the Kramers–Kronig relation,

$$\frac{1}{E_0} - \frac{1}{E_\infty} = \frac{2}{\pi}\int_0^{\infty} d\omega \, \frac{1}{\omega} \mathrm{Im}\frac{1}{E(\omega)},$$

and the fact that $a(v)$ increases slower with v than linear so that $v/a \to \infty$ as $v \to \infty$. Thus, from (C1) we get as $v \to \infty$,

$$G(v,T) \to G_0(\infty,T)\frac{E_\infty}{E_0}.$$

It should be noted that in this equation, $G_0(\infty,T)$ occurs rather than $G_0(0,T)$, which can be understood as follows.[19,20]

Consider a crack in a rectangular slab with clamped upper and lower surfaces (see Fig. 3). The elastic energy stored in a segment Δx far in front of the crack is $U_0\Delta V$, where $\Delta V = \Delta x h_0 w$ is the volume of the segment and $U_0 = \sigma_0^2/2E_0$ is the energy density per unit volume (σ_0 is the applied stress). If the crack moves very slowly, the elastic energy in ΔV will vanish when the crack has moved far ahead of it, so the full energy $U_0\Delta V$ has been used to break the bonds at the crack tip, which gives $U_0\Delta V = G_0(0,T)\Delta x$. Since there is no viscoelastic energy dissipation in this case,

$$G(0,T) = G_0(0,T) = U_0\frac{\Delta V}{\Delta x}. \tag{C2}$$

Now, consider a very fast moving crack. In this case, the solid will respond with its high frequency modulus as the crack-tip pass the segment Δx so the drop in the stored elastic energy will be $U_\infty\Delta V$, where

$$U_\infty = \frac{\sigma_0^2}{2E_\infty} = \frac{E_0}{E_\infty}U_0. \tag{C3}$$

As $v \to \infty$, the remaining energy $(U_0 - U_\infty)\Delta V$ will be dissipated via viscoelastic relaxation when the crack tip is far in front of the volume element and can, therefore, not be used to break the bonds at the crack tip.[20] (For a solid of finite length, the crack my even split the solid into two parts before the viscoelastic relaxation transfer the remaining stored elastic energy into heat.[19]) Hence, for a fast moving crack,

$$U_\infty\Delta V = G_0(\infty,T)\Delta x. \tag{C4}$$

Since the crack propagation energy is determined by the elastic energy stored far in front of the crack tip, and in particular, $G(\infty,T)\Delta x = U_0\Delta V$, using (C3) and (C4), we get $G(\infty,T) = (E_\infty/E_0)G_0(\infty,T)$.

In the treatment above, we have assumed that the effective spring constant K is a constant, which is likely to a good approximation for cohesive cracks but is unlikely to be a valid approximation for adhesive cracks if the viscoelastic factor $[1+f]$ is important.

REFERENCES

[1] *Fatigue Crack Growth in Rubber Materials: Experiments and Modeling*, *Advances in Polymer Science Vol. 286*, edited by G. Heinrich, R. Kipscholl, and R. Stocek (Springer Nature, 2021).
[2] *Degradation of Elastomers in Practice, Experiments and Modeling*, *Advances in Polymer Science Vol. 289*, edited by G. Heinrich, R. Kipscholl, and R. Stocek (Springer Nature, 2023).
[3] A. N. Gent, "Adhesion and strength of viscoelastic solids. Is there a relationship between adhesion and bulk properties?," Langmuir **12**, 4492 (1996).
[4] C. Y. Hui, B. Zhu, and R. Long, "Steady state crack growth in viscoelastic solids: A comparative study," J. Mech. Phys. Solids **159**, 104748 (2022).
[5] M. H. Müser and B. N. J. Persson, "Crack and pull-off dynamics of adhesive, viscoelastic solids," Europhys. Lett. **137**, 36004 (2022).
[6] R. S. Rivlin and A. G. Thomas, "Rupture of rubber. I. Characteristic energy for tearing," J. Polym. Sci. **10**, 291 (1953).
[7] A. Cristiano, A. Marcellan, B. J. Keestra, P. Steeman, and C. Creton, "Fracture of model polyurethane elastomeric networks," J. Polym. Sci., Part B: Polym. Phys. **49**, 355 (2011).
[8] G. Carbone, C. Mandriota, and N. Menga, "Theory of viscoelastic adhesion and friction," Extreme Mech. Lett. **56**, 101877 (2022).
[9] C. Creton and M. Ciccotti, "Fracture and adhesion of soft materials: A review," Rep. Prog. Phys. **79**, 046601 (2016).
[10] T. Horst, K. Reincke, S. Ilisch, G. Heinrich, and W. Grellmann, "Fracture surface statistics of filled elastomers," Phys. Rev. E **80**, 046120 (2009).
[11] E. Barthel, "The linear viscoelastic fracture theory applies to soft solids better when they are. . .viscoelastic," Proc. R. Soc. A **480**, 2288 (2024).
[12] W. G. Knauss, "A review of fracture in viscoelastic materials," Int. J. Fract. **196**, 99 (2015).
[13] R. A. Schapery, "A theory of crack initiation and growth in viscoelastic media," Int. J. Fract. **11**, 141 (1975).
[14] J. A. Greenwood and K. L. Johnson, "The mechanics of adhesion of viscoelastic solids," Philos. Mag. A **43**, 697 (1981).
[15] C. Y. Hui, D. B. Xu, and E. J. Kramer, "A fracture model for a weak interface in a viscoelastic material (small scale yielding analysis)," J. Appl. Phys. **72**, 3294 (1992).
[16] P.-G. de Gennes, "Fracture of a weakly crosslinked adhesive," CR Acad. Sci. II **307**, 1949 (1988).
[17] B. N. J. Persson and E. A. Brener, "Crack propagation in viscoelastic solids," Phys. Rev. E **71**, 036123 (2005).
[18] B. N. J. Persson, O. Albohr, G. Heinrich, and H. Ueba, "Crack propagation in rubber-like materials," J. Phys.: Condens. Matter **17**, R1071 (2005).
[19] B. N. J. Persson, "On opening crack propagation in viscoelastic solids," Tribol. Lett. **69**, 115 (2021).
[20] B. N. J. Persson, "A simple model for viscoelastic crack propagation," Eur. Phys. J. E **44**, 3 (2021).
[21] G. Carbone and B. N. J. Persson, "Hot cracks in rubber: Origin of the giant toughness of rubberlike materials," Phys. Rev. Lett. **95**, 114301 (2005).
[22] G. Carbone and B. N. J. Persson, "Crack motion in viscoelastic solids: The role of the flash temperature," Eur. Phys. J. E **17**, 261 (2005).
[23] C. Mandriota, N. Menga, and G. Carbone, "Enhancement of adhesion strength in viscoelastic unsteady contacts," J. Mech. Phys. Solids **192**, 105826 (2024).
[24] C. Mandriota, N. Menga, and G. Carbone, "Adhesive contact mechanics of viscoelastic materials," Int. J. Solids Struct. **290**, 112685 (2024).
[25] C. Müller and M. H. Müser, "How short-range adhesion slows down crack closure and contact formation," J. Chem. Phys. **159**, 234705 (2023).

[26]A. Papangelo, R. Nazari, and M. Ciavarella, "Friction for a sliding adhesive viscoelastic cylinder: Effect of Maugis parameter," Eur. J. Mech. A Solids **107**, 105348 (2024).
[27]J. Slootman, V. Waltz, C. Yeh, C. Baumann, R. Göstl, J. Comtet, and C. Creton, "Quantifying rate- and temperature-dependent molecular damage in elastomer fracture," Phys. Rev. X **10**, 041045 (2020).
[28]C. Müller, M. Samri, R. Hensel, E. Arzt, and M. H. Müser, "Revealing the coaction of viscous and multistability hysteresis in an adhesive, nominally flat punch: A combined numerical and experimental study," J. Mech. Phys. Solids **174**, 105260 (2023).
[29]There exist two alternative ways to describe thermally activated processes. In the Arrhenius approach[30] the reaction rate is written as $\kappa = \nu_A \exp(-\Delta H/k_B T)$ where the activation energy is the change in the internal energy (or entalphy) ΔH when going from the initial state to the top of the reaction barrier. The prefactor ν_A depends on the vibrational frequencies and damping of the motion as described by the theory of activated processes developed by Kramers.[31] In the Eyring approach[32] the reaction rate is written as $\kappa = \nu_E \exp(-\Delta G/k_B T)$. Here $\Delta G = \Delta H - T\Delta S$ is the free energy of activation to achieve the transition state. The prefactor $\nu_E = k_B T/h$, where h is the Planck constants. The free energy contains an entropic term ΔS in addition to the enthalpic one ΔH. In the Arrhenius equation, this entropic term is accounted for by the pre-exponential factor ν_A, e.g., there will be a vibrational entropy contribution to ν_A. More specifically, $\nu_A = (k_B T/h)\exp(\Delta S/k_B)$. Here we will use the Eyring equation but neglect the entropy term.
[30]S. A. Arrhenius, "Über die Dissociationswärme und den Einfluss der Temperatur auf den Dissociationsgrad der Elektrolyte," Z. Phys. Chem. **4**, 96 (1889).
[31]H. A. Kramers, "Brownian motion in a field of force and the diffusion model of chemical reactions," Physica **7**, 284 (1940).
[32]H. Eyring, "The activated complex in chemical reactions," J. Chem. Phys. **3**, 107 (1935).
[33]L. B. Freund, *Dynamic Fracture Mechanics* (Cambridge University Press, Cambridge, England, 1998).
[34]T. L. Anderson, *Fracture Mechanics: Fundamentals and Applications* (CRC Press, Boca Raton, 1995).
[35]B. Lorenz, B. A. Krick, N. Mulakaluri, M. Smolyakova, S. Dieluweit, W. G. Sawyer, and B. N. J. Persson, "Adhesion: Role of bulk viscoelasticity and surface roughness," J. Phys.: Condens. Matter **25**, 225004 (2013).
[36]A. Maghami, Q. Wang, M. Tricarico, M. Ciavarella, Q. Li, and A. Papangelo, "Bulk and fracture process zone contribution to the rate-dependent adhesion amplification in viscoelastic broad-band materials," J. Mech. Phys. Solids **193**, 105844 (2024).
[37]K. R. VanDonselaar, D. A. Bellido-Aguilar, M. Safaripour, H. Kim, J. J. Watkins, A. J. Crosby, D. C. Webster, and A. B. Croll, "Silicone elastomers and the Persson-Brener adhesion model," J. Chem. Phys. **159**, 184708 (2023).
[38]A. Tiwari, L. Dorogin, A. I. Bennett, K. D. Schulze, W. G. Sawyer, M. Tahir, G. Heinrich, and B. N. J. Persson, "The effect of surface roughness and viscoelasticity on rubber adhesion," Soft Matter **13**, 3602 (2017).
[39]B. N. J. Persson, "Nanoadhesion," Wear **254**, 832 (2003).
[40]G. J. Lake and A. G. Thomas, "The strength of highly elastic materials," Proc. R. Soc. London, Ser. A **300**, 108 (1967).
[41]B. N. J. Persson, *Sliding Friction, Physical Principles and Applications*, 2nd ed. (Springer, 2000).
[42]M. H. Müser, M. Urbakh, and M. O. Robbins, "Statistical mechanics of static and low-velocity kinetic friction," Adv. Chem. Phys. **126**, 187 (2003).
[43]L. Prandtl, "Ein Gedankenmodell zur kinetischen Theorie der festen Körper," Z. Angew. Math. Mech. **8**, 85 (1928).
[44]B. N. J. Persson, *Sliding Friction: Physical Principles and Applications*, 2nd ed. (Springer, Heidelberg, 2000).
[45]M. H. Müser, "Velocity dependence of kinetic friction in the Prandtl-Tomlinson model," Phys. Rev. B **84**, 125419 (2011).
[46]H. Eyring, "Viscosity, plasticity, and diffusion as examples of absolute reaction rates," J. Chem. Phys. **4**, 283 (1936).
[47]E. Evans and K. Ritchie, "Dynamic strength of molecular adhesion bonds," Biophys. J. **72**, 1541 (1997).
[48]R. Merkel, P. Nassoy, A. Leung, K. Ritchie, and E. Evans, "Energy landscapes of receptor-ligand bonds explored with dynamic force spectroscopy," Nature **397**, 50 (1999).
[49]K. Kendall, "Peel adhesion of solid films–The surface and bulk effects," J. Adhes. **5**, 179 (1973).
[50]S. K. Thanawala and M. K. Chaudhury, "Surface modification of silicone elastomer using perfluorinated ether," Langmuir **16**, 1256 (2000).
[51]A. Ghatak, K. Vorvolakos, H. She, D. L. Malotky, and M. K. Chaudhury, "Interfacial rate processes in adhesion and friction," J. Phys. Chem. B **104**, 4018 (2000).
[52]M. K. Chaudhury, "Rate-dependent fracture at adhesive interface," J. Phys. Chem. B **103**, 6562 (1999).
[53]S.-Q. Wang, Z. Fan, C. Gupta, A. Siavoshani, and T. Smith, "Fracture behavior of polymers in plastic and elastomeric states," Macromolecules **57**, 3875 (2024).
[54]S.-Q. Wang and Z. Fan, "Investigating the dependence of elastomeric fracture on temperature and rate," Rubber Chem. Technol. **96**, 530 (2023).
[55]S.-Q. Wang, Z. Fan, A. Siavoshani, M. C. Wang, and J. Wang, "Fresh considerations regarding time-dependent elastomeric fracture" Extreme Mech. Lett. (to be published).
[56]Far in front of the crack-tip the stress field must equal the applied stress σ_0 but in the analyzis we include only the singular part $\sim 1/\sqrt{r}$ of the stress field which will dominate close to the crack tip. This should be a good approximation for a slab of sufficient height h_0 as the stress σ_0 for a given stored elastic energy scales as $\sim 1/\sqrt{h_0}$ with the height h_0 of the slab. The singular part of the stress field close to the crack-tip is usually written as $\sigma_{zz} = K_I/(2\pi\sqrt{r})$, where the stress intensity factor K_I for an opening crack for the configuration shown in Fig. 3(b) (thin plate; plane stress state) is given by $K_I = \sigma_0\sqrt{(h_0/2)}$. This result can be derived using (2) and $G = K_I^2/E$ which is valid for plane stress.
[57]P. L. Piotrowski, R. J. Cannara, G. Gao, J. J. Urban, R. W. Carpick, and J. A. Harrison, "Atomistic factors governing adhesion between diamond, amorphous carbon and model diamond nanocomposite surfaces," J. Adhes. Sci. Technol. **24**, 2471 (2010).
[58]J. Washiyama, E. J. Kramer, C. F. Creton, and C.-Y. Hui, "Chain pullout fracture of polymer interfaces," Macromolecules **27**, 2019 (1994).
[59]B. N. J. Persson, "Model study of brittle fracture of polymers," Phys. Rev. Lett. **81**, 3439 (1998).
[60]B. N. J. Persson, "Fracture of polymers," J. Chem. Phys. **110**, 9713 (1999).
[61]A. Tiwari, L. Dorogin, M. Tahir, K. W. Stöckelhuber, G. Heinrich, N. Espallargas, and B. N. J. Persson, "Rubber contact mechanics: Adhesion, friction and leakage of seals," Soft Matter **13**, 9103 (2017).
[62]H. R. Brown, C.-Y. Hui, and E. Raphael, "Interplay between intermolecular interactions and chain pullout in the adhesion of elastomer," Macromolecules **27**, 608 (1994).
[63]E. Raphael and P. G. de Gennes, "Rubber-rubber adhesion with connector molecules," J. Phys. Chem. **96**, 4002 (1992).
[64]B. N. J. Persson, "On the role of inertia and temperature in continuum and atomistic models of brittle fracture," J. Phys.: Condens. Matter **10**, 10529 (1998).
[65]J. R. Kermode, A. Gleizer, G. Kovel, L. Pastewka, G. Csanyi, D. Sherman, and A. De Vita, "Low speed crack propagation via kink formation and advance on the silicon (110) cleavage plane," Phys. Rev. Lett. **115**, 135501 (2015).
[66]J. Fineberg and M. Marder, "Instability in dynamic fracture," Phys. Rep. **313**, 1 (1999).
[67]B. N. J. Persson and A. I. Volokitin, "Rubber friction on smooth surfaces," Eur. Phys. J. E **21**, 69 (2006).
[68]A. Schallamach, "A theory of dynamic rubber friction," Wear **6**, 375 (1963).
[69]Y. B. Chernyak and A. I. Leonov, "On the theory of the adhesive friction of elastomers," Wear **108**, 105 (1986).
[70]B. Lorenz, Y. R. Oh, S. K. Nam, S. H. Jeon, and B. N. J. Persson, "Rubber friction on road surfaces: Experiment and theory for low sliding speeds," J. Chem. Phys. **142**, 194701 (2015).
[71]A. Tiwari, N. Miyashita, N. Espallargas, and B. N. J. Persson, "Rubber friction: The contribution from the area of real contact," J. Chem. Phys. **148**, 224701 (2018).
[72]K. A. Grosch, "The relation between the friction and visco-elastic properties of rubber," Proc. R. Soc. London, Ser. A **274**, 21 (1963).